

To Mr. Chas. J. McCarthy, Asst. Dir. Mgr.
Vought-Sikorsky Aircraft Div.
United Aircraft Corp

Source of Acquisition
CASI Acquired

NATIONAL ADVISORY COMMITTEE FOR AERONAUTICS

VOUGHT-SIKORSKY AIRCRAFT LIBRARY

THIS DOCUMENT AND EACH AND EVERY
PAGE HEREIN IS HEREBY RECLASSIFIED
FROM Conf TO Unclass.
AS PER LETTER DATED NACA Release,
note #122

SPECIAL REPORT No. 112

RADIATOR DESIGN AND INSTALLATION

By M. J. Brevoort and M. Leifer
Langley Memorial Aeronautical Laboratory

May 1939

5K112

RADIATOR DESIGN AND INSTALLATION

By M. J. Brevoort and M. Leifer

SUMMARY

The fundamental principles of fluid flow, pressure losses, and heat transfer have been presented and analyzed for the case of a smooth tube with fully developed turbulent flow. These equations apply to tubes with large length-diameter ratios where the flow is at a high Reynolds Number. The error introduced by using these equations increases as the magnitude of the tube length and the air-flow Reynolds Number approaches the values encountered in modern radiator designs. Accordingly, heat-transfer tests on radiator sections were made and the results are presented in nondimensional form to facilitate their use and for comparison with other heat-transfer data. In addition, pressure losses were measured along smooth tubes of circular, square, and rectangular cross section and the results were also correlated and are presented in nondimensional form.

The problem of a radiator design for a particular installation is solved, the experimental heat-transfer and pressure-loss data being used, on a basis of power chargeable to the radiator for form drag, for propelling the weight, and for forcing the air through the radiator.

The case of an installation within a wing or an engine nacelle is considered. An illustration of radiator design is carried through for an arbitrary set of conditions. Sufficient detail is given to enable the reader to reproduce the analysis for any given case. The effect upon the cooling efficiency is considered for a change in the following design conditions:

- (1) The pressure drop across the radiator.
- (2) The pump efficiency of the duct.
- (3) The free-area ratio of the radiator.
- (4) The wing characteristics for the design conditions.
- (5) The air constants.
- (6) The change in density with altitude.
- (7) The width of the water passageway.

Comparisons of the cooling efficiency possible with tubes of various shapes lead to the conclusion that the smooth hexagonally shaped tube is superior to the circular tube and that finned tubes and tubes shaped to produce turbulence cause a decrease in cooling efficiency.

The use of ethylene glycol instead of water for the liquid makes it possible to increase the cooling efficiency several times (depending upon the inlet-air temperature). The analysis of the length of passage on the liquid side of the radiator shows it to be a secondary consideration. The design problem for an installation in a separate nacelle is solved. Several values are chosen for the effective nacelle-drag coefficient to permit evaluation of the nacelle-wing interference on the cooling efficiency. A cooling-power comparison between liquid-cooled and air-cooled engines is made and it is concluded that the power to cool is not a determining factor in the selection of the type of engine. The recovery of mechanical energy from the heat energy dissipated by the radiator in the duct is shown to be possible. An approximate determination of the magnitude of the effect is made. The design of the radiator is not affected by considerations of the energy recovery.

INTRODUCTION

With the wealth of information available in heat-transfer processes, all the necessary information for the design of aircraft radiators would appear to be at hand. Such is practically the case. In fact, there is so much information on special cases that a designer setting out to choose a radiator is confused by a large variety of reports, all of which appear to have some bearing on the problem.

The most misleading reports of this type are those dealing with the radiator mounted in the air stream. The data in these reports were invaluable when radiators were mounted outside the airplane without benefit of cowling, but the data apply only to a special case and cannot be used for a modern radiator installation in which the radiator is located in a wing, a cowling, or an engine nacelle.

A radiator mounted in a free air stream acts more or less like a flat plate, depending upon the resistance to flow through the radiator tubes. If the radiator has a

high resistance, most of the air flow approaching the radiator diverges and passes around the outside. In so doing, the air breaks away at both the front and the rear faces of the radiator, resulting in a large drag. If the radiator is made with a low resistance to flow through the tubes, most of the air approaching the radiator goes through the radiator and the drag is greatly reduced.

When the radiator is mounted in the free air stream, the power consumed by the radiator increases with the cube of the velocity. With the radiator in a duct, however, it is necessary to consider only the weight of the radiator and the internal power consumed in it. The radiator located in a duct can be made to dissipate a given amount of heat by almost as low an expenditure of power for cooling as desired. But the lower the power, the larger the radiator. The most economical radiator size depends upon the wing loading of the particular airplane.

There appears to be a prevalent notion that, by the invention of some peculiar tube arrangement and shape, large gains in cooling performance can be attained. The best situation that can be obtained is to have the friction loss that occurs in the radiator be true surface friction on the direct cooling surface. Pressure losses associated with sharp contractions, expansions, and sharp bends as well as surface friction over an indirect cooling surface are all undesirable. If the optimum condition is realized, it appears to be of little importance from considerations of heat dissipation whether the tubes are circular, square, rectangular, hexagonal, or any other convenient shape. One shape may have an advantage over another as regards the ratio of weight required to the space remaining for the liquid flow. If the radiator meets the requirements of direct cooling surface and pressure loss connected only with the surface friction, however, the chief consideration may be the ease of manufacture, the ease of repair, and the durability.

This report will review the fundamental principles of heat transfer as they apply to the problem of radiators. Original data on radiators will be presented and a number of special cases will be analyzed on the basis of the fundamental principles, the data, and similar data from other sources.

SYMBOLS

The following symbols are used in the report and are listed alphabetically for ready reference.

- A, frontal area of the housing.
- A_c , total cooling surface upon which h_t is based.
- c_1, c_2 , constants.
- c_p , specific heat at constant pressure.
- c_v , specific heat at constant volume.
- C_L , lift coefficient of the wing.
- C_{D_w} , drag coefficient of the wing.
- C_{D_n} , drag coefficient of the radiator installation with no cooling-air flow.
- D, hydraulic diameter of the tube.
- D, drag.
- d, radiator depth.
- f_1 , friction factor $\left(\frac{\Delta p D}{q_t 4L}\right)$.
- f, free-area ratio, of open frontal area to the total frontal area.
- g, the acceleration of gravity.
- h, surface heat-transfer coefficient.
- h_t , over-all heat-transfer coefficient from fluid to fluid.
- h_a , heat-transfer coefficient from air to tube wall.
- h_l , heat-transfer coefficient from liquid to tube wall.
- H, quantity of heat dissipated per unit time.

- H_r , required quantity of heat dissipation.
- k , thermal conductivity.
- K_1, K_2, \dots , constants.
- L , tube length.
- M , mass flow of fluid per unit time.
- $Nu = \frac{hD}{k}$, Nusselt number.
- P , power.
- P_t , total power chargeable to the radiator.
- P_D , power required to force the air through the radiator.
- P_W , power required to support and propel the weight of the radiator.
- p , static pressure.
- Δp , total pressure difference, usually across the radiator.
- Δp_f , drop in pressure due to skin friction.
- $Pr = \frac{c_p \mu}{k}$, Prandtl number.
- $q = \frac{1}{2} \rho V^2$, dynamic pressure (q carries same subscripts as V , velocity).
- Q , quantity of air by volume passing through the radiator per unit time.
- $R = \rho \frac{VD}{\mu}$, Reynolds Number.
- R , universal gas constant.
- T , absolute temperature, $^{\circ}F$.
- T_a , air temperature.
- T_{ia} , inlet-air temperature.
- T_w , average liquid temperature.

- $\Delta T_a = T_a - T_{ia}$, change in air temperature.
- ΔT_w , change in liquid temperature.
- ΔT_{w-a} , mean temperature difference between coolant and air.
- V_d , air velocity in the duct.
- V_t , air velocity in the tube.
- V_o , air-stream velocity.
- v , specific volume.
- W , the work obtainable from a cycle.
- w , radiator width.
- W_r , weight of the radiator.
- x , length of tube to the section under consideration.
- ϵ , factor by which to multiply radiator weight to account for the additional required airplane structure.
- γ , ratio of the specific heats of air.
- ρ , density.
- ρ_h , density at altitude h .
- ν , kinematic viscosity.
- η_t , heat-transfer efficiency.
- η_p , pump efficiency of the duct with the radiator installed.
- μ , coefficient of viscosity.

Subscripts:

- i , apply to the inside of the tube.

- o, apply to the outside of the tube.
- O, apply to the free air stream.
- w, apply to the liquid side of the radiator.

SINGLE TUBES

Analysis

A radiator being composed of a number of small tubes, it is essential to have a clear understanding of the operation of the individual tube in a study of radiator characteristics. This statement does not mean that single tubes can be studied and the results applied without qualification to a radiator comprising an assembly of tubes.

Much of the published data on single tubes has been taken for a region of the tube well downstream from the tube entrance and, as a result, gives results that show the frictional losses and the heat transfer for tubes in which the boundary layer is in equilibrium. That is, the boundary layer is either in the laminar condition with parabolic velocity distribution over the tube or is in the completely developed turbulent condition. Now in a radiator tube, if the Reynolds Number is below some critical value, the boundary layer will be laminar and the velocity distribution will go through a continuous evolution from almost uniform at the entrance to parabolic across the section considered. If the tube is less than 150 diameters in length, the tube may be completely in the stabilizing region. It will therefore have a thinner boundary layer and, as a result, a greater friction and consequently a greater heat-transfer coefficient. If the Reynolds Number is above some critical value, the flow in the tube may be turbulent. If the entrance is favorable for initiating turbulence in the flow, the tube will have turbulent flow throughout its length and will have the friction and the heat-transfer coefficients associated with turbulent flow and the particular Reynolds Number. If the entrance is designed to give a smooth streamline flow, the flow will evolve through a transition and become turbulent downstream. The higher the Reynolds Number, the nearer this transition point will be to the tube entrance. Thus it is seen that, even though the flow may be above the critical Reynolds Number, the tube may be too short to give an op-

portunity for the stabilizing flow to break down. If the entrance is such that turbulence is initiated, for a flow above the critical Reynolds Number, the flow will remain turbulent throughout. On the other hand, if the flow is below the critical Reynolds Number, the turbulence set up by an entrance will be damped out and laminar flow will result.

It is now obvious that tests on single tubes have direct application to the radiator problem only when the tubes are tested under conditions reproducing those existing in a radiator. If the entrance to a tube assembly in a radiator is smoothly streamlined, then the heat-transfer coefficient decreases rapidly downstream from the entrance as the boundary layer builds up. It is therefore necessary to study numerous combinations of lengths and diameters to develop the complete picture of the phenomena involved. If the entrance promotes turbulence, however, the friction and the heat-transfer coefficients will closely approximate the accepted results for turbulent flow in tubes.

The pressure loss, or friction, in tubes has been studied by Stanton and others for both the laminar and the turbulent regimes in the regions where the boundary layer is developed. The relations that satisfy each condition are given by Glauert (reference 1) as follows:

$$\frac{dp}{dL} = -32 R^{-1} \rho \frac{V_t^2}{D} \quad \text{for laminar flow} \quad (1)$$

$$\frac{dp}{dL} = -0.157 R^{-\frac{1}{4}} \rho \frac{V_t^2}{D} \quad \text{for turbulent flow} \quad (2)$$

Friction-Loss Tests and Correlation

The pressure losses were measured on circular tubes having diameters of 1/2, 1/4, 1/8, and 1/16 inch; a square tube of 1/2 inch hydraulic diameter; and rectangular tubes 1/2 by 1/8 inch and 1/2 by 1/16 inch. The length of tube was made appropriate to give a length-diameter ratio of 150 to 200 for each tube.

The pressures were measured by static tubes flush with the inside of the tube, as seen in figure 1(a). The

tube surfaces were smooth, and a bell-shape entrance assured streamline flow at the outset (fig. 1(b)). The velocity was measured by a survey using a pitot tube mounted on a micrometer. Typical surveys for the 1/2-inch-diameter circular tube are shown in figure 2. It was found that the entrance was sufficiently close to a streamline shape that the velocity calculated from the first static-tube reading and the atmospheric pressure agreed within the experimental error with the average velocity measured in the survey.

Figure 3 shows a sample curve of the pressure-drop measurements on one of the tubes. The results for all the tubes tested, plotted in nondimensional form, are shown in figure 4; the abscissa is the Reynolds Number, the ordinate is the friction factor f_1 , and each curve is for a constant length-diameter ratio. The data for all the tubes fall on the curves with the exception of the square and the rectangular tubes, which agree in the turbulent region but deviate radically from the data for circular tubes in the laminar region.

From equations (1) and (2), $f_1 = 16/R$ for laminar flow and $f_1 = 0.0785/R^{0.25}$ for turbulent flow. The curves for fully developed laminar and turbulent flow are also shown on figure 4. The test data should fall between the two curves for fully developed flow because the stabilization and the transition regions are included.

The friction-factor data for the radiators tested are shown in figure 5. Data from the single-tube tests at the same L/D ratio as that for the smooth-tube radiators are also plotted. The curves from radiator data should fall higher than the curves from the single-tube data because the radiator Δp includes the losses at the exit. Since the transition occurs at the same Reynolds Number for both tubes and radiators, the exit losses can be determined from the differences between the friction factors for the single tubes and the radiators. Table I illustrates values of the exit loss over a range of Reynolds Numbers. The average exit-loss value for the 1/4-inch-diameter tube is seen to be $0.2 q_t$, in agreement with Hartshorn (reference 2). The larger values found for the 1/8-inch-diameter tube may be attributed to a lower free-area ratio, which results in a greater expansion at the exit, and possibly to the relatively greater soldering irregularities at entrance and exit.

TABLE I
EXIT LOSSES FOR THREE RADIATORS

Radiator	Reynolds Number	Exit loss/ q_t
a _A	6,000	0.19
	15,000	.23
	30,000	.305
B	6,000	0.18
	15,000	.15
	25,000	.12
C	6,000	0.33
	13,000	.435

^a See fig. 5 for explanation of the radiator designations.

A radiator was made up having tube exits faired gradually from a circular to a hexagonal form over a distance of about 1 inch. Although this fairing appreciably reduced the exit loss for the single tube, no measurable improvement was found for the radiator.

Figure 4 may be used to obtain the variation of air velocity in the tube with tube length for any pressure drop and tube diameter. The method is as follows: For any choice of L and D , figure 4 gives the relationship between $f_1 = \Delta p D / q_t 4L$ and Reynolds Number $= \rho V_t D / \mu$. The conditions of temperature and pressure determine ρ and μ . The velocity V_t is calculated from any Reynolds Number and q_t follows. The corresponding value of f_1 gives Δp . Proceeding in this manner gives several sets of values of V_t and Δp . Then V_t is plotted against $(\Delta p + 0.2 q_t)$. The term $0.2 q_t$ is included to account for pressure losses at the radiator exit. (See table I.) Such plots enable the determination of V_t for any over-all pressure drop $(= \Delta p + 0.2 q_t)$. Repeating the process for other lengths or diameters will give the desired relationship between air velocity in the tube and tube length. Figure 6 illustrates this relationship, using the values for D and Δp (over-all) shown on the figure.

The Reynolds Number describes the nature of the boundary layer. Inasmuch as both the friction loss of the fluid and the heat transfer from wall to fluid depend upon the nature of the boundary layer, both characteristics are functions of the Reynolds Number. Reynolds recognized this common dependence on Reynolds Number and stated the dependence in a principle known as Reynolds analogy. As a result

$$h = \frac{f_1 c_p V_t \rho}{2} \quad (3)$$

Both the friction factor and the heat-transfer coefficient are larger with turbulent flow than with laminar flow above the critical Reynolds Number and each is larger with a thin than with a thick boundary layer. A more elaborate relation has been evolved as a result of the work of Stanton, Prandtl, Taylor, and others that correlates the data on heat transfer from pipes for various velocities and fluids; namely,

$$Nu = \frac{hD}{k} = c_1 (Pr)^l (R)^m \left(\frac{L}{D}\right)^n \quad (4)$$

Equation (4) is the equation used by many workers in this field to correlate experimental heat-transfer data. The constant c_1 and the exponents l , m , and n vary with a change in the type of flow. For very long pipes, $(L/D)^n$ can be assimilated into the constant and a new constant c_2 used. The exponent n in any case is small. The term L/D has a strong influence only in the entrance region of the tube where the boundary layer is going through change. The Prandtl number is nearly constant when air is used as the fluid flowing through the tube. It follows then that equation (4) for air flow and a constant L/D reduces to

$$h = c_2 k \frac{R^m}{D} \quad \text{or} \quad c_2 \frac{k V_t^m \rho^m}{D^{1-m} \mu^m} \quad (5)$$

Equations for Heat-Transfer and Cooling-Power Loss

The local heat-transfer coefficient and the friction factor have been related in the foregoing discussion. There remains the problem of determining how much heat can

be dissipated from a given tube as a function of wall temperature, inlet-air temperature, Reynolds Number, and length. Although the average local heat-transfer coefficient can be determined by means of the tube friction, the tube length has an important bearing on the actual heat transfer by controlling the rise in the air temperature. The heat-transfer efficiency η_t has been defined to describe the efficiency of heating up of the air as

$$\eta_t = \frac{\Delta T_a}{T_w - T_{ia}}$$

It is desirable to have a high heat-transfer efficiency in order to dissipate a maximum amount of heat for a given mass flow of air.

The heat dissipated and the power for cooling per unit open frontal area of tube can be determined as a function of Δp , $T_w - T_{ia}$, L , D , and the physical constants of the fluid. The ratio of these two quantities gives a relation from which it will be possible to determine the optimum dimensions.¹

The analysis will be made for the case of fully developed turbulent flow in a tube of constant wall temperature. The tube considered is circular, but the equations may be applied equally well to hexagonal or square tubes by using the hydraulic diameter.

The heat ΔH dissipated for a length dx of the tube (fig. 7) is

$$\Delta H = h (T_w - T_a) \pi D dx \quad (6)$$

Also

$$\Delta H = \rho V_t c_p \frac{\pi D^2}{4} dT_a \quad (7)$$

From equations (6) and (7) it may be shown that

$$\frac{T_a - T_{ia}}{T_w - T_{ia}} = \eta_t = 1 - e^{-\frac{4h}{\rho V_t c_p} \frac{x}{D}} \quad (8)$$

¹This analysis for optimum tube dimensions takes no account of the radiator weight or the profile drag, which will be considered later.

where the heat-transfer efficiency is now expressed as a function of the tube dimensions, the average heat-transfer coefficient, and the mass flow through the tube.

For fully developed turbulent flow, Prandtl, quoted in reference 3 (p. 173), gives

$$h = c_1 c_p \frac{\mu^{0.2}}{D^{0.2}} (\rho V_t)^{0.8} \quad (9)$$

where $c_1 = 0.0269$. From equations (7), (8), and (9), a relation similar to that derived by Hartshorn (reference 2) is found:

$$H = \rho V_t c_p \frac{\pi D^2}{4} (T_w - T_{ia}) \left[1 - e^{-4c_1 \left(\frac{\mu}{D \rho V_t} \right)^{0.2} \frac{L}{D}} \right] \quad (10)$$

where H is given in B.t.u./hr.

ρ , in lb./cu.ft.

V_t , in ft./hr.

h , in B.t.u./hr./°F./sq.ft.

μ , in lb./hr. ft.

Temperatures are in degrees Fahrenheit and lengths are in feet. Hartshorn also developed a very useful family of curves of H per unit frontal area against ρV at various values of L/D .

From equation (2), the velocity is given as

$$V_t = \frac{\Delta p^{0.571} D^{0.714}}{L^{0.571} c_2^{0.571} v^{0.143} \rho^{0.571}} \quad (11)$$

where $c_2 = 0.157$.

Eliminating V_t from equation (10), using equation (11), and taking the units into account, the heat dissipation per unit open frontal area is given as:

$$\frac{H}{\pi D^2/4} = \frac{0.841 \times 10^5 c_p \rho^{0.429} \Delta p^{0.571} D^{0.714} (T_w - T_{ia})}{c_2^{0.571} \nu^{0.143} L^{0.571}} \times \left(1 - e^{-\frac{c_1 c_2^{0.1142} \mu^{0.2} \nu^{0.0285} L^{1.1142}}{2.42 \rho^{0.086} \Delta p^{0.1142} D^{1.343}}} \right) \quad (12)$$

where ν is in ft.²/hr.

Δp , in lb./sq.ft.

Figure 8 shows the variation of the heat dissipated with the length of the tube for a constant Δp for several tube diameters. Figure 9 shows the variation of the heat dissipated with the length of the tube for a tube diameter of 1/48 foot for several values of Δp . It may be noted from figure 8 that the peak heat dissipation per square foot of open area occurs at about the same value of L/D for the various diameters.

Hartshorn (reference 2) showed that the peak efficiency as a function of L/D varied as $D^{0.2}$.

The basis for the choice of a radiator is its cooling efficiency, defined as the ratio of the heat dissipated to the power chargeable to the radiator.

The total power chargeable to the radiator is

$$P_t = C_{D_n} A q_o V_o + \epsilon \frac{C_{D_w}}{C_L} V_o W_r + \frac{Q \Delta p}{\eta_p} \quad (13)$$

On the right side of this equation, the first term is the power to overcome the form drag; the second term is the power to support the weight; and the third term is the power to force the air through the radiator.

The pump efficiency is defined in reference 4 for a separate nacelle installation as

$$\eta_p = \frac{Q \Delta p}{(D - D_o) V_o}$$

The useful cooling work done per second is $Q\Delta p$ and the work expended for cooling is $(D - D_0) V_0$. The quantity D_0 is the drag of a closed cowling with major dimensions similar to those of the actual cowling, and $(D - D_0)$ is the drag increment due to the cooling-air flow.

Similarly, the pump efficiency for a duct is defined as the ratio of the useful cooling work done to the total work expended in forcing the air through the radiator. Thus for a wing duct,

$$\eta_p = \frac{Q\Delta p}{\Delta D V_0}$$

where ΔD is the difference in drag between the original wing and the wing with the duct-radiator combination. In any installation, the entrance and the exit losses are included in the pump efficiency.

The form-drag power is not entirely independent of the cooling-air flow, and the choice of the pump efficiency as an interference factor enables the breakdown of the total power required into the subdivision stated. In an installation where the cooling-air flow may decrease the form drag, the pump efficiency may be more than 100 per cent. It is possible that, for such cases, the basic shape without cooling-air flow may be considerably improved and such considerations may be worth investigating.

It is likely that the pump efficiency will vary with the flight speed and the quantity of cooling-air flow.

For the radiator mounted in a separate nacelle, the results presented in reference 4 give C_{D_n} and η_p ; the airplane design determines C_{D_w} and C_L .

For the radiator mounted inside an engine nacelle or within a wing, the first term on the right side of equation (13) vanishes. This fact makes the installation within a wing very attractive because, without the frontal-area limitation, it is only necessary to seek a compromise between the second and the third terms. The best compromise results in an installation with a more favorable cooling efficiency than is possible when a separate nacelle installation is used.

RADIATORS

Apparatus for Heat Transfer

The heat dissipation of several radiators was studied. Circular tubes were used for the following radiators:

- (1) Length, 9 inches; tube diameter, 0.250 inch.
- (2) Length, 18 inches; tube diameter, 0.240 inch.
- (3) Length, 5 inches; tube diameter, 0.125 inch.

In addition, a radiator was built up of corrugated tubing (fig. 10) with a length of 1.97 feet and a mean diameter of 0.41 inch. For these four radiators, air was passed through the tubes and water was directed perpendicular to them. The average inlet and outlet temperatures of both the air and the water were measured by means of thermocouples. The mass flow of air was obtained either by a survey using a pitot tube and static tubes in the duct downstream from the radiator or, more commonly, by a venturi connecting the air at room temperature and atmospheric pressure with a large box, or expansion chamber, ahead of the radiator duct. The mass flow of water was obtained from a calibrated orifice in the water line. The pressure drop across the radiator was measured by pitot and static tubes connected to an alcohol manometer. The apparatus for the heat-transfer investigation is shown in figure 11.

In the results herein presented, the actual average value of the local heat-transfer coefficient from air to tube wall h_a is used. In order to obtain an accurate value of this coefficient, the water passages were made short and the water velocity was kept high so that the drop in temperature of the water ΔT_w was very small. Several water speeds were used at each air speed, and the over-all heat-transfer coefficient h_t was plotted against $\Delta T_w / \Delta T_a$, as in figure 12, where each curve is for a constant mass flow of air. The curves were extrapolated to $\Delta T_w / \Delta T_a = 0$. At this value, $1/h_t = 0$, where h_l is the heat-transfer coefficient from liquid to tube wall. Since

$$\frac{1}{h_t} = \frac{1}{h_a} + \frac{1}{h_l}$$

then $h_a = h_t$. The value of h_t was computed in all cases using the logarithmic mean temperature difference from air to water.

Heat-Transfer Data

The formula for the heat-transfer coefficient given by McAdams (reference 3, p. 173) is for completely developed turbulent flow. Figure 13 shows the heat-transfer data, plotted in nondimensional form, obtained from several typical radiators compared with the McAdams formula. Except for the corrugated-tube radiator, the radiators tested showed a lower heat-transfer coefficient than indicated by the formula for turbulent flow. The same general formula can be used, however, for radiators at Reynolds Numbers above 10,000 by changing the coefficient from 0.0269 to 0.0247. Similarly, Hartshorn (reference 2) analyzed the data of Lorenz (reference 5) and found the coefficient equal to 0.026. Care must be used in the following sections to apply the data and the equations to regions where they will be valid.

The heat-transfer coefficient was found to be lower than that for turbulent flow given by McAdams and Hartshorn (fig. 13). This difference was to be expected inasmuch as the friction loss was also less. (See fig. 4.) The explanation lies in the entrance conditions for the flow. At Reynolds Numbers in the usual operating range of a radiator, an appreciable length of the tube is in the stabilization region where the flow is neither laminar nor turbulent. Thus the friction factor and the heat-transfer coefficient should fall between the curves for established laminar and turbulent flow.

The empirical equations presented earlier based on a turbulent boundary layer will give both too high a heat transfer and too high a power consumption to push the air through the radiator. Almost the same optimum dimensions will be found for the radiator regardless of whether these equations or the present experimental results are used.

INSTALLATION WITHIN A WING OR AN ENGINE NACELLE

The high cost of cooling commonly associated with liquid cooling was due almost entirely to the radiator installation. The radiator was located in the air stream without benefit of cowling and with no means of controlling the cooling. The drag was large, owing to the large frontal area, and the cooling power increased with the cube of the air speed. If the radiator gave adequate cooling in climb, too much cooling was available at cruising. Radiators have been made retractable and have been mounted in the engine nacelle, in the wing, or in separate nacelles. Each of these arrangements has lowered the power required for cooling. The cost of cooling can be reduced to a fraction of that required in present installations by a properly designed arrangement.

When the radiator is installed within a wing or an engine nacelle, the power chargeable to the radiator is composed of two parts: the power actually used in cooling P_D , which is given by $Q\Delta p/\eta_p$; and the power used to carry and propel the weight of the radiator and water P_W , which is given by $\epsilon (C_{D_w}/C_L) W_r V_o$. The results of these considerations will be presented on the basis of optimum heat dissipation with respect to the power dissipated for various tube lengths and diameters.

For the following case, several variables will be kept fixed in order to simplify the discussion. Later these variables will be changed one by one to ascertain their importance and effect. The design Δp is taken as 25.6 pounds per square foot; the entrance and exit losses for each radiator are taken as 0.2 qt; the pump efficiency for the duct is taken as 100 percent; the ratio of open to total frontal area f is taken as 0.650; $\epsilon (C_{D_w}/C_L) = 0.1$; the fluid is water, $T_w - T_{ia} = 70^\circ \text{ F.}$; the tube-wall thickness is 0.005 inch; and the density, the specific heat, and the viscosity of the air are taken at 73.5° F.

The necessary data are obtained from figures 4 and 13. Figure 4 is used to give the variation of tube velocity with tube length for $\Delta p = 25.6 \text{ lb./sq.ft.}$ and several tube diameters, as previously explained. Then, by means of equation (10) with V_t from figure 6 and the heat-

transfer data from figure 13 (equivalent to putting $c_1 = 0.0247$ in equation (10)), curves of $\frac{H}{\pi D^2/4}$ against length for the assumed conditions are plotted in figure 14.

Figure 14 differs from figure 8 in several respects. The data for figure 8 were obtained from the empirical equations for fully developed turbulent flow, whereas the data for figure 14 are the results of measurements under the actual flow conditions. In addition, the exit loss is included in the pressure losses used to obtain figure 14, but the exit loss was not considered for figure 8.

The Selection of Optimum Radiator Dimensions

The power expended for cooling is equal to $Q\Delta p$, or

$$P_D = Q\Delta p = \frac{(\pi D^2/4) V_t \Delta p}{\pi D^2/4} = V_t \Delta p \text{ foot-pounds per square}$$

foot of open frontal area.

The design Δp , 25.6 pounds per square foot, together with the velocities from figure 6, gives the power for cooling for any tube length and diameter.

The power expended in carrying and propelling the weight of the complete radiator is a function of the flight speed, the aerodynamic characteristics of the airplane, and the type of radiator. That is, $P_W = \epsilon (C_{D_W}/C_L) W_r V_0$; $\epsilon (C_{D_W}/C_L) = 0.1$; and $V_0 = 200$ and 300 miles per hour for the illustration. The remaining variable, W_r , may be approximately computed for round or hexagonal tubes as a function of L/D , of length, and of the free-area ratio. (See the appendix.) The method is found to check the weights of the radiators used by Harris and Caygill (reference 6) within 2 or 3 pounds per square foot of frontal area. This variation is about that encountered in manufacture.

If the heat dissipated is divided by the sum of the powers expended for cooling and weight propulsion for a particular tube diameter and length, figure 15 is obtained, showing the variation of $\frac{H}{P_D + P_W}$ against length, for three diameters and two air speeds.

Figure 15 is the solution to the problem for the previously mentioned conditions. Table II compares the optimum values of these curves for an energy dissipation of 500 horsepower. It is now of interest to investigate the effect of variations in these conditions.

TABLE II

A COMPARISON OF THE OPTIMUM RADIATOR-DESIGN
SOLUTIONS OF FIGURE 15

[Energy to be dissipated, 500 hp.; $T_w - T_{ia} = 70^\circ \text{ F.}$;
 Δp , 25.6 lb./sq.ft.; f , 0.650; $\epsilon (C_{D_w}/C_{L})$, 0.1]

V_o (m.p.h.)	D (ft.)	L (ft.)	$\frac{L}{D}$	$\frac{H}{\pi D^2/4}$ (hp./sq. ft. open frontal area)	$\frac{H}{P_D + P_W}$	Power used $P_D + P_W$ (hp./sq.ft. open frontal area)	Frontal area required (sq.ft.)
200	1/96	0.58	55.7	111.6	11.92	41.9	6.89
	1/48	1.105	53.0	112.6	9.82	50.9	6.82
	1/32	1.50	48.0	107.6	8.31	60.2	7.14
300	1/96	0.52	50.0	109.6	9.83	50.9	7.01
	1/48	.90	43.2	107.6	7.96	62.8	7.14
	1/32	1.30	41.6	102.5	6.68	74.8	7.50

The Choice of Δp

The Δp chosen for the design is fundamental in determining the relative cooling efficiency of the radiator. In any particular problem it will be necessary to determine beforehand the value of the pressure drop to be used in the radiator design. An upper limit is set by the climbing speed of the airplane. The lower limit is determined by the amount of space available for the duct and the radiator.

The choice of the design Δp is made as follows: A particular tube diameter is taken as fixed. Then, for each Δp considered, the tube velocity, the heat transfer, the power used for cooling, and the power used for weight propulsion are calculated for a series of values of L . The conditions assumed and the calculations are shown in table III. Table III is used to construct figure 16(a),

showing a plot of cooling efficiency $\frac{H}{P_D + P_W}$ against length for the various values of Δp . The optimum length and the cooling efficiency for each value of Δp from this figure are used to construct table IV, which compares the various values of Δp on the basis of the power and the frontal area required to dissipate 500 horsepower. Data for $\Delta p = 6.4$ lb./sq. ft. are taken from figures 6 and 14. Figure 16(b) is then drawn, the values from table IV being used. From figure 16(b) it is evident that the choice of Δp to result in an optimum cooling efficiency will be determined by the space limitations of the wing or the engine nacelle. Although a fixed pump efficiency has been used in these calculations, a decreased pump efficiency will probably be associated with large velocity reductions in the duct entrance section. A similar set of curves will result for any other tube diameter since the optimum values of figure 16(a) are primarily a function of L/D . Hence, the Δp chosen from considerations of one tube diameter will serve satisfactorily for the design pressure drop.

TABLE IV

A COMPARISON OF THE OPTIMUM VALUES FROM FIGURE 16(a)

[Energy to be dissipated, 500 hp.; $T_w - T_{ia} = 70^\circ \text{ F.}$;
 $f, 0.750$; $\eta_p, 100$ percent; $\epsilon (C_{D_w}/C_{L}), 0.1$;
 $V_o, 300$ m.p.h.; $D, 1/48$ ft.]

Δp (lb./sq.ft.)	L (ft.)	$\frac{H}{P_D + P_W}$	$\frac{H}{\pi D^2/4}$ (hp.)	Power required $P_D + P_W$ (hp.)	Frontal area required (sq. ft.)
6.4	0.36	10.70	38.5	46.7	13.00
25.6	.98	8.80	111.2	56.8	5.99
40.0	1.25	7.63	144.0	65.5	4.63
64.0	1.74	6.25	187.5	80.0	3.55
100.0	2.00	4.98	237.2	100.5	2.81

It is apparent from table IV that the cooling efficiency increases as the Δp decreases. These cooling efficiencies are, however, for radiators of varying lengths. Accordingly, computations were made to ascertain the variation of cooling efficiency for a given radiator as the Δp changes over a wide range. For this purpose, equations (6) and (8) were combined to give

$$\frac{H}{\pi D^2/4} = g \rho V_t c_p (T_w - T_{ia}) \left(1 - e^{-\frac{4h}{\rho V_t c_p g} \frac{L}{D}} \right)$$

where H is given in B.t.u./sec.

V_t , in f.p.s.

ρ , in slugs/cu. ft.

g , in ft./sec.²

The data for V_t and h for each value of Δp are ob-

tained from figures 4 and 13, respectively. Figure 17 shows the cooling efficiency $\frac{H}{P_D + P_W}$ plotted against Δp for a standard-type radiator under the conditions given in the figure. It is seen that the cooling efficiency reaches a maximum at a Δp of 13.5 pounds per square foot for the stated conditions, whereas the cooling efficiency for the optimum design at each Δp (fig. 16(b)) increased with decreasing Δp as long as the type of flow remained unchanged.

The Variation in Pump Efficiency

Figure 18 shows the effect of reducing the pump efficiency from 100 to 80 percent. In this case, the power expended for cooling, $Q\Delta p/\eta_p$, is increased; the efficiency of cooling is reduced; and the peak of the curve is moved in the direction of longer tube lengths. Harris and Recant (reference 7) present data on pump efficiency for wing ducts.

Variation of the Ratio of Open to Frontal Area, f

The heat dissipation per square foot of open frontal area is, of course, unaffected. The variation of f introduces two important changes, both of which affect the weight of the radiator. An increase in f will decrease the water capacity of the radiator and the frontal area for any required quantity of heat dissipation. The maximum value of f for a particular tube will be discussed on the basis of a minimum desirable water-passage width.

Somewhat arbitrarily, the minimum water-passage width is set at 0.028 inch in order to assure open waterways and a moderate expenditure of power for pumping. The thickness of the tube metal is taken as 0.005 inch. The free-area ratio for these conditions can now be calculated from geometric considerations. (See table V.)

TABLE V

THE EFFECT OF TUBE SHAPE AND SIZE UPON THE FREE-AREA RATIO

[Wall thickness, 0.005 in.; minimum water-passage width, 0.028 in.]

Radiator	Tube shape	Inside diameter (ft.)	Free-area ratio, f
A	Round	1/96	0.465
B	do.	1/48	.60
C	do.	1/32	.65
D	Hexagonal	1/96	.59
E	do.	1/48	.75
F	do.	1/32	.83

The diameter for the hexagonal tube is the distance across the flats, equal to the hydraulic diameter.

Figure 19 shows the variation of cooling efficiency with length for these radiators. Table VI lists these radiators at the peak values. The corrugated-tube radiator is included for comparison.

On the basis of this analysis, the hexagonal tube is shown to be superior to the round tube. Neither tube appears to have any advantage from a consideration of ease of construction.

The Effect of Variation in C_{D_w}/C_L

The power used to carry the weight of the radiator is $\epsilon (C_{D_w}/C_L) W_r V_o$. Thus a variation in C_{D_w}/C_L will produce exactly the same effect as a proportional variation in V_o . Figure 15 gives the plot of $\frac{H}{P_D + P_W}$ against length for velocities of 200 and 300 miles per hour with $\epsilon (C_{D_w}/C_L)$ constant at 0.1. The same figure can be used to show the variation of $\epsilon (C_{D_w}/C_L)$ by keeping $V_o = 200$

miles per hour and giving $\epsilon (C_{D_w}/C_L)$ the value of 0.1 for the upper curve and of 0.15 for the lower curve or, alternately, by keeping $V_0 = 300$ miles per hour and giving $\epsilon (C_{D_w}/C_L)$ the value of 0.1 for the lower curve and of 0.067 for the upper curve. Inasmuch as the value of $\epsilon (C_{D_w}/C_L)$ is fixed by the particular airplane considered, it will affect the design considerations only as it affects the value of the tube length for the maximum cooling efficiency. This fact is illustrated in figure 15, the curves being interpreted as suggested.

The Effect of Changes in the Air Constants Due to Heating

The effect on the heat dissipated.— Consider equation (10) in the following form:

$$\frac{H}{\pi D^2/4} = \rho V_t c_p (T_w - T_{ia}) \left[1 - e^{-4c_1 \frac{\mu^{0.2}}{D^{0.2}} \frac{1}{(\rho V_t)^{0.2}} \frac{L}{D}} \right] \quad (10)$$

The change in c_p with temperature is negligible.

Consider the effect of a change in the value of the viscosity μ . A change in air temperature from 32° F. to 122° F. will change μ from 0.0172 to 0.0193, about 2 percent in $\mu^{0.2}$. Thus, by taking an average value for μ , the change would be about 1 percent in the exponent. The maximum value of H and the L/D for the maximum value are not affected. For values of L/D below 35, however, the heat dissipation increases by about 1 percent. For values of L/D over 40, the effect is a fraction of 1 percent and can be neglected.

In equation (10), the density occurs only in the combination ρV_t . Therefore, if the mass flow of air through the radiator is kept constant, the variation in ρ due to heating will not affect the heat transfer because ρV_t will not change. This condition of constant mass air flow will necessitate an increase in the pressure drop across the radiator with a corresponding change in the power required for cooling.

The effect on the power for cooling.— For a heated

radiator, the pressure drop across the radiator is equal to the difference in total pressure (fig. 20):

$$\begin{aligned}\Delta p &= p_1 + \frac{1}{2} \rho_1 u_1^2 - (p_2 + \frac{1}{2} \rho_2 u_2^2) \\ &= p_1 - p_2 - f^2 \left(\frac{1}{2} \rho_2 V_2^2 - \frac{1}{2} \rho_1 V_1^2 \right) \quad (\text{neglecting end losses}) \\ &= p_1 - p_2 - \frac{\rho_1 V_1^2}{2} f^2 \left(\frac{T_2 P_1}{T_1 P_2} - 1 \right) \quad (14)\end{aligned}$$

where the variation in ρ due to heating and pressure change along the tube is considered. The pressure effect being present for a cold radiator, it will not be included in the corrections.

According to the momentum theorem,

$$p_1 - p_2 = \Delta p_f + (\rho_2 V_2^2 - \rho_1 V_1^2)$$

where Δp_f is the drop in pressure due to skin friction

$$= \Delta p_f + \rho_1 V_1^2 \left(\frac{T_2 P_1}{T_1 P_2} - 1 \right) \quad (15)$$

Then

$$\begin{aligned}\Delta p &= \Delta p_f + \rho_1 V_1^2 \left(\frac{T_2}{T_1} - 1 \right) \left(1 - \frac{f^2}{2} \right) \\ &\quad + \text{an end loss } 0.1 \rho_2 V_2^2 \quad (16)\end{aligned}$$

neglecting the pressure change along the tube. The change in Δp upon heating the radiator and keeping ρV constant arises from the terms on the right-hand side of equation (16). The increased velocity of the air in the tube will result in a larger pressure loss due to skin friction. The second term on the right represents the increase in pressure drop as a result of an addition of momentum to the air in passing through the radiator. A small portion of this added momentum is converted into total pressure, reducing the momentum pressure drop by a factor $f^2/2$. Finally, the end loss slightly increases by reason of the higher value of the exit velocity.

Lorenz (reference 5) finds that, for various values

of $T_w - T_{ia}$, the value of $\Delta p_f/q_t$ remains constant and equal to that for the cold radiator. Then, since $\Delta p_f/q_t$ is constant for the various radiator temperatures,

$$(\Delta p_f)_{\text{heated}} \left(\sim \frac{1}{2} \rho V^2 \right)_{\text{mean}} \sim \frac{1}{2} \rho_1 V_1^2 \frac{\rho_1}{\rho_{\text{mean}}}$$

using $\rho_1 V_1 = \rho_2 V_2 = \rho_{\text{mean}} V_{\text{mean}}$. This relationship will give the increase in Δp_f for a given change in the density of the air with sufficient accuracy for design purposes. Capon (reference 8) shows from theoretical considerations that, for values of L/D of about 40, the increase in the skin-friction term is about 0.3 the momentum term. No data are available for longer tube lengths.

The magnitude of the effect may be computed for one of the radiators tested: Consider a radiator with $L = 5$ inches, $D = 1/8$ inch, $L/D = 40$, $f = 0.6$. Take the initial conditions at 73.5° F. with $V_1 = 130$ feet per second. Then

$V_1 = 130 \text{ f.p.s.}$	and taking $\Delta T_a = 27^\circ \text{ F.}$,	$T_2 = 560^\circ \text{ F. absolute}$
$\rho_1 = 0.00231$	using $\rho_1 V_1 = \rho_2 V_2$	$\rho_2 = 0.00220$
$v_1 = 1.67 \times 10^{-4}$		$V_2 = 136.5 \text{ f.p.s.}$
$T_1 = 533^\circ \text{ F. absolute}$		$v_2 = 1.84 \times 10^{-4}$

Then

$$q_1 = 19.5 \text{ lb./sq.ft.}$$

$$q_2 = 20.5 \text{ lb./sq.ft.}$$

$$\text{End loss}_1 = 3.9 \text{ lb./sq.ft.}$$

$$\text{End loss}_2 = 4.1 \text{ lb./sq.ft.}$$

$$\text{Momentum change} = \rho_1 V_1^2$$

$$\left(\frac{T_2}{T_1} - 1 \right) \left(1 - \frac{f^2}{2} \right)$$

$$= 1.6 \text{ lb./sq.ft.}$$

$$R_1 = 8,110$$

$$\frac{\Delta p}{q} = 1.10 \text{ (by fig. 4)}$$

$$(\Delta p_f)_1 = 21.5 \text{ lb./sq.ft.} \quad (\Delta p_f)_{\text{heated}} = 22.0 \text{ lb./sq.ft.}$$

$$\Delta p_1 \text{ total} = 25.4 \text{ lb./sq.ft. (cold)} \quad \Delta p_2 \text{ total} = 27.7 \text{ lb./sq.ft. (heated)}$$

The calculated change in pressure is 9.0 percent. The observed increase is about 6 percent.

The condition of constant mass air flow, assumed to simplify the foregoing discussion, caused a change in the Δp required. From design considerations, the available pressure drop is the independent variable. It is necessary to start with this quantity to compute the mass air flow and, finally, the power required for cooling.

From equation (16), it follows that the increase in pressure caused by heating the radiator is

$$\rho_1 V_1^2 \left(\frac{T_2}{T_1} - 1 \right) \left(1.1 - \frac{f^2}{2} \right) + (\Delta p_f)_1 \left(\frac{T_2 - T_1}{T_2 + T_1} \right) \quad (17)$$

Figure 4 will provide the velocity of the air in the tube V_1 for a given available Δp . Equation (17) will then give the increase in the pressure drop after correcting for the temperature rise expected. Figures similar to 6, 14, and 15 are then constructed, using the reduced Δp for a cold radiator. As previously explained, the mass flow of air calculated for the cold radiator at the reduced Δp will remain as the mass air flow for the hot radiator at the given Δp . In the calculation of the P_D or $V_t \Delta p$, the Δp used is the actual pressure drop and $V_t = \frac{V_1 + V_2}{2}$. In the computation of the cooling efficiency for figure 15, the power for cooling is added to the power for carrying the weight of the radiator.

The Effect of a Change in Altitude upon the Radiator Efficiency

Meredith (reference 9) in an analysis of the effect of altitude on cooling efficiency found the density as a function of the temperature. This function varies with the coolant and the initial temperature difference. Any solution of the problem is based on the standard atmos-

phere (reference 10), which itself is standard only under rarely realized specified atmospheric conditions.

A general method of ascertaining the effect of altitude upon the radiator performance for a supercharged engine is needed. For the case of a constant duct-exit opening, it is possible to evaluate the decrease in heat dissipation under specific flight conditions for increasing altitudes.

Equation (10) is used in the following form:

$$\frac{\bar{H}}{\pi D^2/4} = 2.75 \times 10^4 \rho V_t (T_w - T_{ia}) \left[1 - e^{-0.00960 \left(\frac{\mu}{\rho V_t D} \right)^{0.2} \frac{L}{D}} \right]$$

where

$\frac{\bar{H}}{\pi D^2/4}$ is in B.t.u./hr./sq.ft. of open frontal area.

ρ , in slugs/cu.ft.

V_t , in f.p.s.

μ , in lb./hr. ft.

The problem reduces to obtaining the variation of μ , ρ , $T_w - T_{ia}$, and V_t with altitude; equation (10) is then used for the heat dissipation. The value for the air density at altitude may be corrected for the adiabatic compression in the duct before the radiator. The conversion of dynamic pressure to static pressure within the duct increases the air density and the temperature of the air. (The quantitative increase in the temperature of the air is later discussed in the section entitled The Jet-Propulsion Effect.)

For the particular airplane, it is necessary to know the variation of velocity with altitude and the velocity of the air in the tube for the design altitude and conditions. For a constant duct-exit opening, V_t is directly proportional to V_0 . Hence, the variation of V_t and ρV_t with altitude may be computed.

The quantity $T_w - T_{ia}$ varies with altitude and the coolant used. By a combination of the foregoing data, the heat dissipation may be obtained for any altitude, as shown by the following example.

The radiator is designed for sea-level operation; $D = 1/48$ foot, $L/D = 50$, $V_t = 150$ f.p.s. It is desired to determine the variation of heat dissipation with altitude at a constant exit setting for level flight at maximum speed. The performance calculations give the variation of flight velocity V_o with altitude, as shown in figure 21. Next, the variation of V_t with altitude is computed. In the computation of ρV_t at altitude, the value of ρ for the free air stream is used. With water as coolant and T_w taken at 27° F. below the boiling temperature at the particular altitude, $T_w - T_{ia}$ is easily obtained. Similarly, with glycol as coolant, T_w is taken at 52° F. below the boiling point for a 97-percent glycol solution. The values for T_{ia} are for the standard atmosphere. The necessary calculations are shown in table VII. The change in heat dissipation with altitude is plotted in figure 22 for both the water and the glycol radiators. The decrease in heat dissipation with altitude is not so serious above the rated altitude because, after that point, the required amount of heat dissipation decreases.

With a constant exit setting, the decrease in heat dissipation with increase in altitude is greater for a glycol radiator than for a water radiator. The reason for this difference is that the variation of air temperature with altitude makes a larger percentage change in the temperature difference between air and coolant for the water radiator than for the glycol radiator.

The Δp required for a constant rate of heat dissipation was calculated by means of equation (12) and is shown in table VII. In addition, the required velocity of the air in the tube, the power for cooling, and the cooling efficiency for a constant rate of heat dissipation are shown. An examination of these columns will readily show the importance of designing the radiator for conditions approximating those to be encountered in operation. For example, the power used for cooling will have doubled at 20,000 feet for the glycol radiator even with the assumption that the pump efficiency has remained constant. The increase in $\Delta p_r/q_o$ with altitude may cause difficulty in dissipating the required amount of heat after a certain altitude. Table VII is not intended to give a comparison of the altitude performance characteristics for water and glycol radiators. The same design was chosen

for both coolants to facilitate computation of table VII, and neither design is optimum for the conditions assumed.

The preceding calculations neglected the corrections to the inlet-air temperature and density for the adiabatic compression in the duct-entrance section. Where only relative values for the heat dissipation at altitude are required, the use of the uncorrected values introduces very little error.

SHAPE OF THE INDIVIDUAL TUBE

The tests on single tubes showed that square and rectangular tubes had the same frictional resistance in the turbulent region as round tubes of the same hydraulic diameter. It is safe to predict, then, that the heat dissipation for the square, hexagonal, or rectangular tubes will also be the same as for the round tubes. Indeed, the heat-transfer equations given for single tubes may be applied to the noncircular tubes by using their hydraulic diameters. The only differences that should appear with variously shaped tubes should be in the heat transfer from liquid to tube wall, the power required to force the liquid through the radiator, the weight of the radiator filled, the end losses, and the free-area ratio.

For example, radiators formed of hexagonal or rectangular tubes, which have uniform liquid passages, will be lighter on account of smaller liquid capacity, will require less frontal area, and may require more power to force the liquid through the radiator. Of these effects, the ones of greatest importance - liquid capacity and frontal area - have been considered under the section Installation within a Wing or an Engine Nacelle.

Some radiators have been built with irregularly shaped air passages, such as the corrugated tubes shown in figure 10. Such shapes are used in an attempt to produce greater mixing of the hot air near the tube wall with the central core of air. Obviously, the desired result can be easily accomplished in a variety of ways.

The variation of the heat-transfer coefficient with Reynolds Number for the corrugated-tube radiator is shown in figure 13. In order to apply the formulas and to compare this radiator with the other types tested, each tube

is considered to have a square cross section with side a . Then $a = 0.410$ inch and $L = 23.7$ inches. In addition, figure 5 shows the isothermal friction factor for this radiator as a function of the Reynolds Number.

For a Δp of 25.6 pounds per square foot, the heat dissipation per unit open frontal area as a function of length is given by figure 14. It is evident that, for equal values of L/D or equal lengths, the corrugated-tube radiator is definitely inferior in heat-dissipating ability.

The low value of the air velocity through the tube reduces the Reynolds Number to such an extent that the effect of the higher value of the heat-transfer coefficient for a given Reynolds Number is nullified and the heat dissipation is reduced. Table VI compares the cooling efficiencies for a corrugated-tube radiator with several circular- and hexagonal-tube radiators under the same conditions.

CONDITIONS OF FLOW AROUND THE TUBES

In the material in the section Single Tubes, the variables affecting friction loss and heat transfer were considered for the inside of the tube. The phenomena involved for the outside of the tube must also be considered. The same fundamental principles rule in the transfer of heat from the liquid to the outside of the tube as from the tube to the fluid on the inside. The liquid may flow perpendicular or parallel to the tubes.

The fact that the same phenomena of friction loss and heat transfer exist for the outside of the tubes as for the inside would appear to make conditions on the outside as much of a problem for study as conditions on the inside. The over-all heat-transfer coefficient h_t from liquid to air is given by

$$\frac{1}{h_t} = \frac{1}{h_a} + \frac{1}{h_l} \quad (18)$$

If either h_a or h_l is small, the total thermal resistance $1/h_t$ is largely determined by that particular term. In most liquid-to-air radiators, $1/h_a$ is much

larger than $1/h_l$ and $1/h_l$ can be neglected. It may easily happen that, with low liquid velocities, h_l will become small enough so that the thermal resistance $1/h_l$ will be important.

In the foregoing radiator design, h_a is taken equal to h_t , and a method of computing the tube length and the number of tubes for each particular case is given. In addition, a certain water-passage width is taken as optimum. Thus, for the chosen tube diameter, the frontal area of the radiator is fixed. Since no conditions have been postulated concerning the arrangement of this required frontal area into any particular form, it follows that the width and the depth (fig. 23(a)) may be varied to fit a desired installation within the limitation that the product wd is constant (fig. 23(b)). Considerations of the water flow around the tubes, however, lead to the establishment of criterions for maximum permissible values for either w or d .

The quantity of heat dissipated for a particular design is determined by the over-all heat-transfer coefficient and the temperature difference between the two fluids. In order to maintain a constant heat dissipation for increasing values of w , it is necessary to maintain both h_t and T_w constant. Further consideration will show that the constancy of h_t necessitates the constancy of ΔT_w . For example, suppose h_t constant as ΔT_w decreases with a greater radiator width. The decrease in ΔT_w implies a decrease in the quantity of heat lost by the water, whereas the increase in the average water temperature T_w increases the water-air temperature difference and hence the quantity of heat dissipated ($= h_t \Delta T_{w-a} A_c$) also increases. The further assumption is herein made that the volume of water flow is constant for the given design heat-transfer conditions.

No investigations have been reported on the variation of the heat-transfer coefficient with Reynolds Number for liquids flowing perpendicular to tube banks of round or hexagonal tubes at the low Reynolds Numbers found in radiators. The present heat-transfer data, when round tubes are used, indicate a Nusselt number of about 65 at a Reynolds Number of 880 based on the water velocity at the minimum passage width and the tube diameter for the length parameter. The Nusselt number may then be roughly assumed

to be directly proportional to the Reynolds Number. Thus, h_l may be calculated for any value of w . Since h_a is known from the design solution, it is possible to estimate the effect upon h_t and, accordingly, upon the heat dissipated for any increase in w .

For long liquid passages or greater radiator depths, h_l becomes increasingly greater than h_a . As previously explained, the increase in h_l does not affect the overall heat-transfer coefficient. The only limitation to be considered is the power expended in pumping the water through the radiator.

TYPE OF LIQUID

The type of liquid enters the problem by its effect on the heat-transfer coefficient, that is, through the Nusselt, Prandtl, and Reynolds Numbers. From the relations shown earlier, the specific heat, the thermal conductivity, the viscosity, and the density of the liquid are the most important variables. Brown and Barlow (reference 11) show that water gives about 6 to 8 percent better heat transfer than glycol. Equal flow rates of water and glycol were used and no correction was made for the diminished air flow due to the higher temperatures at which the radiator was operated. Since the diminished air flow decreased h_a by several percent and since higher liquid-flow rates are possible with glycol at equal pump speeds (reference 12) it appears that the dimensions of the radiator and the velocity of flow can be made more suitable to the glycol and can reduce the 6 percent as much as desired.

The heat-transfer coefficient h_l from liquid to the tube wall will vary in the same manner as h_a from air to tube wall. Thus

$$\frac{h_l D}{k} \propto \left(\frac{c_p \mu}{k} \right)^n \left(\frac{\rho V_t D}{\mu} \right)^m \quad (19)$$

where values of $n = 0.3$ and $m = 0.5$ are taken for flow below the critical Reynolds Number from McAdams (reference 3, ch. VIII). Various experimenters have found values of n and m differing from 0.3 and 0.5 over a limited range.

The average values chosen will serve sufficiently well for the discussion. Then

$$h_l \propto \frac{c_p^{0.3} \rho^{0.5} k^{0.7}}{\mu^{0.2}} \quad (20)$$

at 194° F.,

ρ_{glycol} is about 1.1 ρ_{water} .

$c_{p \text{ glycol}}$ is about 0.62 $c_{p \text{ water}}$.

k_{glycol} is about 0.45 k_{water} .

μ_{glycol} is about equal to μ_{water} .

Then

$$\frac{h_{\text{water}}}{h_{\text{glycol}}} = \left(\frac{1}{0.62}\right)^{0.3} \left(\frac{1}{1.1}\right)^{0.5} \left(\frac{1}{0.45}\right)^{0.7} = 1.92$$

In the normal operation of a radiator, $h_l = 50 h_a$ when water is the liquid. Then

$$\frac{1}{h_t} = \frac{1}{h_l} + \frac{1}{h_a} = \frac{1}{50 h_a} + \frac{1}{h_a}$$

$$h_t = \frac{50}{51} h_a$$

Thus, if h_l becomes several times as large, the effect on h_t , which is the determining factor, is negligible. If h_l is only half as large, $h_t = 25/26 h_a$, and the difference is 2 percent in h_t . Thus, by the use of glycol, the over-all heat-transfer coefficient at the same volume of liquid flow is 2 percent less than for water. The available temperature difference $T_w - T_{ia}$ with glycol is several times that for water, depending on the inlet-air temperature, so that the net result is several times the total heat transfer with the same air flow and liquid flow. The cooling efficiency may be still further increased, for

the total available duct space, being adequate for the water radiator at a certain Δp , will now permit the glycol radiator to function at a lower Δp with the desired result.

INSTALLATION IN A SEPARATE NACELLE

In the consideration of the installation of the radiator in a separate nacelle, previous considerations of power used for cooling and weight support apply. It is only necessary to add the power lost owing to propelling the nacelle without any cooling air flow through the nacelle. It follows from equation (13) and the previous discussion that, for a required amount of heat dissipation,

$$P_t = (P_D + P_W) \frac{H_r \pi D^2}{H} + \frac{C_{D_n} q_o V_o}{550} \frac{H_r \pi D^2}{fH} \frac{\pi D^2}{4}$$

$$= \left[P_D + P_W + \frac{C_{D_n} q_o V_o}{550 f} \right] \frac{H_r \pi D^2}{H} \frac{\pi D^2}{4} \quad (21)$$

Subscript 0 refers to the free air stream and P_D and P_W refer to unit open frontal area.

The Choice of Δp

The cooling efficiency improved with a decrease in the pressure drop for a radiator mounted in a wing or an engine nacelle. A radiator mounted in a separate nacelle, however, has an optimum Δp , which is fully as important as the optimum radiator dimensions. For any particular tube diameter and flight conditions, the comparison can be worked out in exactly the same manner that was previously followed in Installation within a Wing or an Engine Nacelle. The value of C_{D_n} for the particular nacelle considered is used. For the present comparison, a well-designed cowling is assumed for which C_{D_n} is 0.12 (reference 4). The power expended in overcoming the form drag per square foot of open frontal area for the conditions in table III with the air at standard density is, from equation (21), 29.5 horsepower. This value is combined with the data of table III and figure 24 is constructed showing the variation of the cooling efficiency

$$\frac{H}{P_t} = \frac{H}{P_D + P_W + \frac{C_{D_n} q_o V_o}{550 f}}$$

with length for several values of Δp . It appears that, for any given installation, one value of Δp will give a maximum cooling efficiency.

The Choice of the Tube Dimensions

Figure 25 shows the variation of the cooling efficiency H/P_t with length for various tube sizes and shapes for three values for C_{D_n} , two of which allow for the interference effect between the wing and the nacelle.

Table VIII shows the values of L/D for the peak cooling efficiencies from figure 25. Considerable latitude is permissible owing to the flat peaks of the curves. Obviously, since the interference effect is very favorable, the same L/D is nearly equally good for all the interference factors computed.

It may be noted that, when the interference effect is moderate or negligible, there appears to be an optimum diameter as well as an optimum length.

For any required amount of heat dissipation, the power required for the radiator is obtained by dividing the required heat dissipation by the cooling efficiency.

TABLE VIII

RADIATOR LENGTHS REQUIRED FOR THE PEAK COOLING EFFICIENCIES

[$T_w - T_{ia} = 70^\circ \text{ F.}$; Δp , 25.6 lb./sq.ft.;
 f , optimum for each tube shape and size; η_p , 100 percent;
 $\epsilon(C_{D_w}/C_L)$, 0.1; V_o , 200 m.p.h.]

Radiator	D (ft.)	Installation							
		In a duct		In a separate nacelle					
				L (ft.)			L/D		
		L (ft.)	L/D	C_{D_n}	$0.40C_{D_n}$	$0.15C_{D_n}$	C_{D_n}	$0.40C_{D_n}$	$0.15C_{D_n}$
A	1/96	0.52	49.9	0.60	0.59	0.52	57.6	56.6	49.9
B	1/48	1.04	49.9	1.25	1.14	1.06	60.0	54.7	50.9
C	1/32	1.46	46.7	1.75	1.62	1.47	56.0	51.8	47.0
D	1/96	.56	53.8	.62	.60	.56	59.5	57.6	53.8
E	1/48	1.15	55.2	1.30	1.20	1.18	62.4	57.6	56.6
F	1/32	1.60	51.2	1.96	1.70	1.64	62.8	54.4	52.5

The actual cooling efficiencies presented in this report are somewhat misleading owing to the small value (70° F.) assumed for $T_w - T_{ia}$. In actual practice, the value of $T_w - T_{ia}$ will be two or three times the design value, increasing the heat dissipation by the same factor. Accordingly, the cooling efficiency will be two to three times as large. A radiator designed from the values in this report giving a cooling efficiency of, say, 7 will actually give a cooling efficiency of 14 to 21; that is, for every horsepower of heat to be dissipated, 1/14 to 1/21 horsepower will be required, or approximately 3.5 to 2.4 percent of the brake horsepower will be used for cooling. The importance of a high-temperature coolant liquid is evident, for the cooling efficiency is directly proportional to the initial temperature difference.

The Cooling Efficiency for a Radiator in a Free Air Stream

The radiator chosen for the comparison is made up of hexagonal tubes having a hydraulic diameter of 0.06 inch and a length of 3.74 inches. The heat-transfer and drag data are given by Parsons and Harper (reference 13) for air speeds of 60 and 120 miles per hour. Extrapolation was made to a flight speed of 200 miles per hour. The power used to transport the weight was calculated, as for the ducted radiator. It is found that, at 200 miles per hour, with $T_w - T_{ia} = 70^\circ \text{ F.}$ and $\epsilon (C_{D_w}/C_L) = 0.1$, the cooling efficiency is about 1.7. Since the same radiator is designed to dissipate an equal or a greater amount of heat in climb at a much lower speed, it is assumed that the radiator is retractable so that this cooling efficiency will hold. For a nonretractable radiator, the cooling efficiency would be much less in addition to the overcooling that would occur. This efficiency is about one-fourth that found in a separate nacelle and becomes rapidly less as the velocity of the airplane increases.

COOLING-POWER COMPARISON OF LIQUID-COOLED AND AIR-COOLED ENGINES

It would appear that the liquid-cooled engine has several inherent advantages. The radiator can be made large, thus allowing cooling at a small Δp and, since the power is proportional to $\Delta p^{3/2}$, this power may be reduced to any desired value. It has been shown, however, that there is a limitation imposed by the power to transport the radiator. The liquid-cooled engine is often pictured as completely enclosed in the wing or the nacelle with no form drag chargeable to the engine installation.

The air-cooled engine, on the other hand, is described as located in a cowl with a large form drag. Now, if the wing is large enough to house the liquid-cooled engine, it is also large enough to house the air-cooled engine. It has been shown (reference 14) that the interference effect between wing and nacelle is favorable so that the effective drag of the nacelle in front of a wing is only 40 percent of the nacelle drag alone. When it is considered that, in these tests, the ratio of the nacelle diameter to wing thickness was large and that the conductivity of the engine was also large, it seems reasonable to assume that

the interference on a modern engine with modern cowling located in a wing of thickness comparable with the engine diameter will be so favorable that the nacelle drag will almost disappear. It is probable that the 40 percent found in the tests of reference 14 will be reduced to the order of 10 percent on a set-up of the nature assumed in this paper.

It was found in reference 4 that the drag of a nacelle of 52-inch diameter at 100 miles per hour was 45 pounds without cooling-air flow and that a streamline nose gave a drag of 32 pounds. It was further found that the engine could be cooled with an additional drag of 20 pounds at this speed. The cooling drag will remain the same regardless of wing thickness. If the interference is favorable, as has been assumed, the form drag reduces to 4.5 pounds so that the total drag at 100 miles per hour is 24.5 pounds; that is, 5.3 horsepower for cooling and 1.2 horsepower for form drag.

With a well-designed cowling, the cooling power at higher speeds will not increase and may possibly decrease. At 300 miles per hour, there is still 5.3 horsepower for cooling and 27 times as much power, or 32 horsepower, for form drag. This form drag is independent of the engine power and depends only on the engine diameter. The cooling power is proportional to the engine power. The values cited are for a 550-horsepower engine. Thus, a 2,000-horsepower engine of the same diameter at 100 miles per hour takes 19.3 horsepower for cooling and 1.2 horsepower for form drag and, at 300 miles per hour, it takes 19.3 horsepower for cooling and 32 horsepower for form drag. This total makes the power required for the engine installation and cooling only 2.5 percent of the engine power.

The power to cool and to transport the cooling system is so small with either liquid- or air-cooled engines that it can hardly be a determining factor in the selection of one in preference to the other.

If the engines are mounted in nacelles in front of comparatively thin wings, the liquid-cooled engine may have a streamline nose, thus having a drag of 32 pounds instead of 45 pounds at 100 miles per hour. A separate nacelle or installation for the radiator, however, will be required, which will add easily as much as this difference in drag.

THE JET-PROPULSION EFFECT

The effect of heating an air stream after expansion in a duct and then contracting the duct before expulsion of the air is to convert some of the added heat energy into thrust. Both Meredith (reference 9) and Capon (reference 8) have made estimates of the thrust so derived.

Neither Meredith nor Capon considers the weight or the form drag of the radiator. If the weight and the form drag are considered, the net effect is a reduction in the power chargeable to the radiator.

In both of the foregoing cases and in the following discussion, losses occurring at the duct entrance and exit are not considered. The question of an efficient duct design is extremely important in the consideration of the propulsive effect, for an inefficient duct will more than offset any possible thrust to be so derived.

The path traversed by the air through the duct shown in figure 26 is illustrated by the path ABCD on the *p-v* diagram in figure 27. The points A, B, C, and D correspond to the positions marked on figure 26.

Path AB represents the adiabatic compression of the air entering the duct. Path BC represents the heating at constant pressure along the duct. Path CD represents the adiabatic expansion as the duct contracts after the heating section. Finally, path DA, representing cooling at constant pressure, is equivalent to expelling the heated air at atmospheric pressure and taking in other air at the same pressure and atmospheric temperature.

When no heat is added, the air traverses the cycle AB, BA, and no work is done. For the cycle ABCD, the work done is

$$\begin{aligned}
 W &= \frac{1}{\gamma - 1} (p_0 v_0 - p_1 v_1) + p_1 (v_2 - v_1) + \frac{1}{\gamma - 1} (p_1 v_2 - p_3 v_3) \\
 &\quad + p_0 (v_0 - v_3) \\
 &= \frac{\gamma}{\gamma - 1} (p_1 v_2 + p_0 v_0 - p_1 v_1 - p_0 v_3) \qquad (22)
 \end{aligned}$$

Using $pv = RT$,

$$W = \frac{RY}{\gamma - 1} (T_2 + T_0 - T_1 - T_3) \quad (23)$$

The heat added per unit mass is

$$H = c_p (T_2 - T_1) \quad (24)$$

The efficiency of the conversion of heat energy into mechanical energy is

$$\frac{W}{H} = \frac{RY}{(\gamma - 1) c_p} \left(1 - \frac{T_3 - T_0}{T_2 - T_1} \right)$$

which gives, using the adiabatic relation

$$\left(\frac{p_0}{p_1} \right)^{\frac{\gamma-1}{\gamma}} = \frac{T_0}{T_1} = \frac{T_3}{T_2} \quad (25)$$

and the relation $R = c_p - c_v$,

$$\frac{W}{H} = \left(1 - \frac{T_3}{T_2} \right) = \left[1 - \left(\frac{p_0}{p_1} \right)^{\frac{\gamma-1}{\gamma}} \right] \quad (26)$$

a result already given by Meredith (reference 9).

Most of the mechanical energy is recoverable as thrust energy. The ratio of the thrust energy to the total mechanical energy, per unit mass of air, is

$$\frac{V_0 (V_3 - V_0)}{\frac{1}{2} (V_3^2 - V_0^2)} = \frac{2V_0}{V_0 + V_3}$$

For example, take $V_0 = 300$ miles per hour and $V_3 = 328$ miles per hour; the useful thrust energy then represents 95.5 percent of the mechanical energy obtained.

In practice, the heat is added by a radiator that requires a certain pressure drop for the heat dissipation. The assumption of constant pressure heating must be altered.

Path BC (fig. 27) is replaced by some path BC', with a decrease in the area of the cycle indicating a reduced conversion of heat into mechanical energy. In order to ascertain the effect of radiator design upon the propulsive effect, the heat will still be considered added at constant pressure, this pressure being taken as the average over the radiator.

Then for $V_0 = 300$ miles per hour at sea level and standard atmospheric conditions, $p_0 = 2,116$ pounds per square foot and $q_0 = 230.4$ pounds per square foot. The design Δp is taken as 25.6 or 64 pounds per square foot. The respective efficiencies are obtained, using equation (26) with $\gamma = 1.4$:

$$1 - \left(\frac{p_0}{p_0 + q_0 - \frac{\Delta p}{2}} \right)^{\frac{\gamma-1}{\gamma}} = 2.8 \text{ and } 2.6 \text{ percent of the heat dissipated converted into mechanical energy.}$$

It has been previously shown that, for any installation, there is a Δp which will permit cooling at a minimum power expenditure. In the radiator design, the only factor that affects the energy recovery is this drop in pressure across the radiator; the lower the pressure drop, the greater the recovery. For the installation in a wing or an engine nacelle, the lowest possible value of the Δp is used for design. Hence a further decrease in the Δp to increase the energy recovery is impossible. For the installation in a separate nacelle, the optimum Δp is used for design. (See fig. 24.) Whereas a change in Δp from 64 to 25.6 pounds per square foot will change the energy recovered from 26 to 28 horsepower for a 1,000-horsepower dissipation, the cooling efficiency decreases by 15 percent or about 12 to 15 horsepower for a good design. To attempt a compromise would reduce the energy recovery to a negligible amount with a real increase in the power expenditure. The conclusion follows that a good radiator design without consideration of the thrust will also be the best design when the thrust effect is taken into account.

As pointed out by Meredith (reference 9), the adiabatic compression of the air entering the duct causes a rise in air temperature. The available temperature difference $T_w - T_{ia}$ will be less than the value using the

atmospheric temperature by an amount depending on the air speed. From equation (25), assuming the air brought to rest,

$$\left(\frac{p_o + \frac{1}{2} \rho v_o^2}{p_o} \right)^{\frac{\gamma-1}{\gamma}} = \frac{T_1}{T_o}$$

gives the upper limit for the temperature rise. Meredith gives the same result in the simple form

$$\Delta T(^{\circ}\text{C.}) = \left(\frac{V_{\text{mph}}}{100} \right)^2$$

CONCLUSIONS

1. The design of a radiator is a function of the conditions under which the radiator is to operate. Hence it is necessary to know beforehand:

- (a) The quantity of heat to be dissipated.
- (b) The available space for an internal installation,
or
- (c) The drag coefficient of the nacelle when no cooling air flow is permitted, in the case of an external installation in a separate nacelle.
- (d) The Δp available in climb.
- (e) The type of liquid, water or glycol, and the value of $T_w - T_{ia}$ expected.
- (f) The probable pump efficiency of the duct or the nacelle installation.
- (g) The ratio of the lift and the drag coefficients of the wing.
- (h) The total weight of the radiator and the additional structure for any radiator dimensions.
- (i) The velocity of the airplane in level flight.

Such information is both necessary and, when combined with the heat-transfer and the pressure-loss data of this report, is sufficient for an optimum radiator design. Particular cases may add other qualifications, such as maximum possible radiator length, a maximum Δp for design to insure good cooling on the ground, etc.

2. The effect of each of the following factors on the cooling efficiency and the radiator dimensions was considered.

(a) The pump efficiency: A decrease in the pump efficiency of the duct will proportionally increase the power for cooling and decrease the cooling efficiency.

(b) The free-area ratio: An increase in the value of the free-area ratio will decrease the radiator weight and the total frontal area with a corresponding increase in the cooling efficiency.

(c) The ratio $\epsilon (C_{D_w}/C_L)$: The power used to transport the radiator weight is directly proportional to the value of $\epsilon (C_{D_w}/C_L)$.

(d) The change in the air constants, c_p , μ , and ρ due to the heating up of the air: To maintain a fixed rate of heat dissipation requires the condition of a constant mass flow of air when the radiator is heated. This requirement in turn necessitates a larger Δp than is required by the same air flow for the isothermal flow. The design solution includes this effect by working out the isothermal case at a reduced Δp . The calculation of the expected increase in Δp caused by heating the radiator is presented.

(e) The change in the heat dissipation with altitude: For a supercharged engine in which the maximum required heat dissipation is at the rated height, an increase in the air flow through the duct is required if the radiator is designed for ground-level conditions. The radiator must be designed with a view to the rated altitude at which it is to operate because the proportion of the available Δp required for cooling increases with altitude.

(f) The width of the water passage: It is desirable to use the smallest possible water-passage width, conditioned upon the power used to pump the liquid through the radiator and the necessity of keeping the water passages open, in order to reduce the radiator weight and to increase the free-area ratio.

A variation in any of the foregoing factors increasing or decreasing any part of the power chargeable to the radiator will cause a change in the optimum radiator dimensions tending to bring the various opposing power considerations into balance again. For example, suppose the pump efficiency decreases. Then P_D increases and the optimum radiator design for the new conditions will have a longer length. The velocity for any given Δp will be less and the value of P_D will be decreased.

3. The fundamental data presented on heat transfer and pressure losses for smooth-tube radiators were obtained for the flow conditions that actually exist in the tube section containing the entrance. A comparison with the established results for fully developed turbulent flow showed that the heat transfer at a particular Δp is about the same for both cases with a larger power expenditure required to force the air through the radiator for the actual flow.

4. An efficient radiator installation within a duct or nacelle where the quantity of flow is controllable is superior to any installation where the radiator is exposed to the air stream, whether the radiator is retractable or shuttered. Relative cooling efficiencies for the installations under similar assumed conditions were as follows:

<u>Installation</u>	<u>Relative cooling efficiency</u>
Retractable radiator	1.7
Separate nacelle	5.9 ... No wing-nacelle interference
Separate nacelle	8.0 ... 40 percent C_{D_n}
Internal duct	9.8

5. In the design of a radiator for an installation within a wing duct or an engine nacelle, it was found that a higher cooling efficiency is possible with a decrease in the Δp across the radiator. Hence, the first step in such a design is to select a value for the Δp that will require a radiator filling all the available frontal area in the duct space. This Δp will be the optimum and minimum for the particular case.

6. The optimum design Δp for an installation within a separate nacelle is the result of a compromise between the powers used for cooling, weight propulsion, and form drag. This case approaches the design problem for a duct as the effective drag coefficient of the nacelle decreases and the power used to overcome the form drag becomes of decreasing importance. On the other hand, as the form-drag power increases in relative magnitude, the frontal area must be decreased, requiring a larger Δp and a longer radiator, thus increasing the power for cooling and the weight propulsion. The best design is in the region where the opposing considerations are of equal importance.

7. The L/D values for the solutions of a radiator-design problem, different tube diameters being used, fall very near each other. Hence, the length available for the radiator is a secondary factor since a reduction in the radiator design length merely calls for the use of a smaller tube diameter. In many cases, one tube diameter will give a slightly higher cooling efficiency than is possible with any other diameter; this solution will be theoretically the most desirable, although perhaps not practicable owing to the length necessary.

8. A comparison was made between the circular tube and the hexagonal tube. It was found that:

(a) The weight of the radiator required for a necessary heat dissipation is lower for a hexagonal tube because the water content of the radiator is less for equal minimum water-passage widths.

(b) The free-area ratio is much higher for a hexagonal tube. Since both shapes have equal heat dissipating ability per square foot of open frontal area, the necessary frontal area will be less for a hexagonal tube. This fact may be used to advantage in the light of conclusions (5) and (6).

9. The higher temperature differences available between liquid and air, when glycol is substituted for water as the coolant, increase the total heat transfer several times, depending on the inlet-air temperature. The decrease in the over-all heat-transfer coefficient when glycol is substituted for water is shown to be several percent. The net result is an increase in heat dissipation per unit frontal area of the radiator. The consequent space saving for any required amount of heat dissipation may be used to decrease the power required to overcome the form drag and the power used in propelling the weight or, alternately, the radiator size may be kept unchanged and the cooling accomplished at a lower Δp with a saving in the power for cooling. In the design process, the balance between the various powers is automatically taken into account by the selection of the optimum design.

10. A comparison of the cooling efficiencies for the air-cooled and the liquid-cooled engines was made. It was shown that the power used for cooling and weight propulsion is of comparable magnitude for both cases and is too small in either case to be used as a determining factor in the selection of one engine over the other.

11. It was found that, at high speeds, a mechanical-energy recovery is possible from the heat dissipated by the radiator in the duct. In the ideal frictionless case, most of this mechanical energy is usefully converted into thrust energy. Good radiator design and energy recovery are compatible for an installation within a wing. For the installation in a separate nacelle, the detrimental effect of changing the design to increase the thrust effect is relatively too great to permit any compromise.

Langley Memorial Aeronautical Laboratory,
National Advisory Committee for Aeronautics,
Langley Field, Va., December 20, 1938.

APPENDIX

THE CALCULATION OF RADIATOR WEIGHTS

The weight of a radiator may be divided into the weight of the tubes, the water within the radiator, the headers (filled), and the solder used to join the tubes at each end.

1. The tube material is taken to be copper of specific weight 555 pounds per cubic foot and the tube-wall thickness is 0.005 inch. Then the weight of the tubes per unit open frontal area =

$$= 555 \times \frac{0.005}{12} \times \frac{\pi D L}{\pi D^2/4} \quad (\text{round tubes})$$

$$= 555 \times \frac{0.005}{12} \times \frac{2\sqrt{3}DL}{\frac{\sqrt{3}}{2} D^2} \quad (\text{hexagonal tubes})$$

units not checked

$$= 0.926 \times \frac{L}{D} \text{ pound} \quad (\text{either shape})$$

2. The weight of the water in the radiator is equal to the density of the water multiplied by the volume remaining after the volume of the tubes and metal is deducted from the total volume. If f is the free-area ratio, then $1/f$ represents the total frontal area per unit open frontal area. Thus, the weight of the water per square foot of open area

$$= 62.4 L \left(\frac{1}{f} - 1 - \frac{\pi D \times \frac{0.005}{12}}{\pi D^2/4} \right) \quad (\text{round tubes})$$

$$= 62.4 L \left(\frac{1}{f} - 1 - \frac{0.005}{3D} \right) \quad (\text{round or hexagonal tubes})$$

3. The data of references 6 and 15 were analyzed to give the relationship between the weight of the headers filled and the tube length. Figure 28 shows the data and the curve used to obtain casing weights for the present report. The radiators of Harris and Caygill (reference 6)

had a frontal area of 1 square foot. Then, per square foot of open frontal area, the casing weight from figure 28 is multiplied by $\sqrt{1/f}$ on the assumption that the casing size increases with the square root of the frontal area. A small error is introduced when the total weight per square foot of open frontal area is used to compute weights for radiators of increasing frontal areas, because the casing weight is now multiplied by the ratio of the frontal areas instead of by the square root of this ratio.

4. The weight of solder per square foot of open frontal area is taken as 1.5 pounds.

REFERENCES

1. Glauert, H.: The Elements of Aerofoil and Airscrew Theory. Cambridge University Press, 1930, pp. 107-108.
2. Hartshorn, A. S.: Note on Performance Data for Honeycomb Radiators in a Duct. R. & M. No. 1740, British A.R.C., 1936.
3. McAdams, William H.: Heat Transmission. McGraw-Hill Book Co., Inc., 1933.
4. Theodorsen, Theodore, Breevoort, M. J., and Stickle, George W.: Full-Scale Tests of N.A.C.A. Cowlings. T.R. No. 592, N.A.C.A., 1937.
5. Lorenz, H.: Wärmeabgabe und Widerstand von Kühler-elementen. Aerod. Inst. an der Tech. Hochs. Aachen, Heft 13, 1933, S. 12-39.
6. Harris, R. G., and Caygill, L. E.: Further Experiments on Honeycomb Radiators. R. & M. No. 952, British A.R.C., 1925.
7. Harris, Thomas A., and Recant, Isidore G.: Investigation in the 7- by 10-Foot Wind Tunnel of Ducts for Cooling Radiators within an Airplane Wing. T.R. (to be published), N.A.C.A., 1939.
8. Capon, R. S.: The Cowling of Cooling Systems. R. & M. No. 1702, British A.R.C., 1936.

9. Meredith, F. W.: Note on the Cooling of Aircraft Engines with Special Reference to Ethylene Glycol Radiators Enclosed in Ducts. R. & M. No. 1683, British A.R.C., 1936.
10. Brombacher, W. G.: Altitude-Pressure Tables Based on the United States Standard Atmosphere. T.R. No. 538, N.A.C.A., 1935.
11. Brown, C. Anderton, and Barlow, F. G.: Heat Dissipation of Ethylene Glycol Radiators and Comparison with Water Radiators. R. & M. No. 1696, British A.R.C., 1936.
12. Pye, D. R.: The Internal Combustion Engine. Vol. II. The Aero-Engine. Oxford at the Clarendon Press, 1934, p. 209.
13. Parsons, S. R., and Harper, D. R., 3d: Radiators for Aircraft Engines. Tech. Paper No. 211, vol. 16, National Bur. Standards, 1922.
14. Wood, Donald H.: Tests of Nacelle-Propeller Combinations in Various Positions with Reference to Wings. Part I. Thick Wing - N.A.C.A. Cowled Nacelle - Tractor Propeller. T.R. No. 415, N.A.C.A., 1932.
15. Harris, R. G., and Alford, W. K.: Wind Channel Tests on Radiators. R. & M. No. 934, British A.R.C., 1925.

TABLE III
THE CALCULATIONS REQUIRED FOR A CHOICE OF Δp

[Hexagonal tube; computations based on unit open frontal area; $T_w - T_{1a} = 70^\circ\text{F.}$; $f, 0.750$;
 $\eta_p, 100$ percent; $\epsilon(C_{D_w}/C_{L})$, 0.1; $V_o, 300$ m.p.h.; $D, 1/48$ ft.; $T_a, 73.5^\circ\text{F.}$]

L (ft.)	L/D	w_r (lb.)	$\frac{F_w}{C_D} = \frac{W}{C_L V_o}$ (hp.)	$\Delta p=25.6$ lb./sq.ft.			$\Delta p=40$ lb./sq. ft.			$\Delta p=64$ lb./sq.ft.			$\Delta p=100$ lb./sq.ft.		
				V_t (f.p.s.)	$\frac{H}{\pi D^2/4}$ (hp.)	P_D (hp.)	V_t (f.p.s.)	$\frac{H}{\pi D^2/4}$ (hp.)	P_D (hp.)	V_t (f.p.s.)	$\frac{H}{\pi D^2/4}$ (hp.)	P_D (hp.)	V_t (f.p.s.)	$\frac{H}{\pi D^2/4}$ (hp.)	P_D (hp.)
0.75	36	63.4	5.07	148.7	102.1	6.92	187.0	123.9	13.60	240.0	153.3	27.9	304.0	186.5	55.3
1.00	48	84.0	6.72	129.0	112.0	6.00	164.0	138.0	11.93	210.5	170.0	24.5	266.0	208.0	48.4
1.25	60	104.4	8.34	113.2	115.5	5.26	145.0	144.0	10.55	187.5	180.0	21.8	239.0	221.5	43.5
1.50	72	125.4	10.04	102.3	117.9	4.76	131.0	147.0	9.52	170.0	185.0	19.8	218.3	231.0	39.7
2.00	96	167.0	13.35	87.9	119.0	4.09	112.5	149.0	8.18	146.0	188.3	17.0	188.5	237.2	34.3

TABLE VI

OPTIMUM COOLING EFFICIENCIES FOR VARIOUS RADIATORS

[Energy to be dissipated, 250 hp.; tube-wall thickness, 0.005 in.; minimum water-passage width,
0.028 in.; $T_w - T_{1a} = 70^\circ\text{F.}$; $\Delta p, 25.6$ lb./sq. ft.; $\eta_p, 100$ percent; $\epsilon(C_{D_w}/C_{L})$, 0.1; $V_o, 200$ m.p.h.]

Radiator	L (ft.)	L/D	Heat dissipated per sq. ft. of open frontal area (hp.)	Required frontal area (sq.ft.)	^a Weight of complete radiator (lb.)	Power required for cooling P_D (hp.)	Power required for weight P_W (hp.)	Total power required P_t (hp.)	Cooling efficiency (neglecting frontal area) $\frac{H}{P_D + P_W}$
A	0.52	50.0	110.0	4.88	215	12.25	11.50	23.75	10.50
B	1.04	50.0	111.5	3.74	251	13.15	13.40	26.55	9.40
C	1.48	47.4	107.0	3.60	295	14.40	15.75	30.15	8.33
D	.56	53.8	111.2	3.81	190	11.70	10.15	21.85	11.45
E	1.17	56.2	114.0	2.92	215	12.05	11.45	23.50	10.70
F	1.65	52.8	110.5	2.73	240	13.20	12.80	26.00	9.61
Corrugated $f = 0.82$	1.30	38.0	72.7	4.19	291	14.7	15.5	30.2	8.28

^aNeglecting decrease in casing weight as the total radiator size increases.

Altitude (ft.)	q_0 (lb./sq.ft.)	μ (lb./hr.ft.)	ρV_t ($\frac{\text{slugs}}{\text{ft.}^2 \text{ sec.}}$)	Water									
				$T_w - T_{ia}$ (°F.)	H (with fixed exit setting) (B.t.u./hr.)	Δp (with fixed exit setting) (lb./sq.ft.)	Δp_r required for constant heat dissipation (lb./sq.ft.)	$\frac{\Delta p_r}{q_0}$	V_t required (f.p.s.)	P_D (hp.)	$\frac{H}{P_D}$		
a.	0	120	0.043	0.357	126	6.10×10^5	42.0	42.0	0.350	150	11.5	20.9	a.
b.	5,000	116	.042	.326	135	6.02	40.6	41.7	.359	161	12.2	19.7	b.
c.	10,000	111	.041	.294	143	5.83	38.8	42.5	.383	175	13.5	17.8	c.
d.	15,000	105	.0395	.264	152	5.59	36.8	43.8	.417	192	15.3	15.7	d.
e.	20,000	97	.0385	.234	160	5.31	34.0	44.9	.463	212	17.3	13.9	e.
f.	25,000	89	.0375	.206	169	5.02	31.2	46.1	.518	234	19.6	12.3	f.
g.	30,000	80	.037	.179	178	4.67	28.0	47.8	.598	262	22.8	10.5	g.
h.	35,000	71	.036	.153	186	4.25	24.8	51.1	.720	297	27.6	8.7	h.
i.	40,000	58	.036	.123	178	3.36	20.3	66.9	1.15	383	46.6	5.2	i.

	Glycol								
	$T_w - T_{ia}$ (°F.)	H (with fixed exit setting) (B.t.u./hr.)	Δp (with fixed exit setting) (lb./sq.ft.)	Δp_r required for constant heat dissipation (lb./sq.ft.)	$\frac{\Delta p_r}{q_0}$	V_t required (f.p.s.)	P_D (hp.)	$\frac{H}{P_D}$	
a.	231	11.2×10^5	46.5	46.5	0.388	150	12.7	34.7	a.
b.	243	10.85	44.8	47.7	.411	164	14.2	31.0	b.
c.	251	10.2	42.8	51.6	.465	184	17.3	25.4	c.
d.	258	9.50	40.5	56.3	.536	208	21.3	20.6	d.
e.	265	8.78	37.4	60.8	.627	242	26.7	16.5	e.
f.	272	8.08	34.3	65.9	.740	267	32.0	13.8	f.
g.	279	7.34	30.9	71.9	.899	306	40.0	11.0	g.
h.	286	6.54	27.4	80.4	1.13	354	51.8	8.5	h.
i.	276	5.20	22.4	104	1.79	454	85.9	5.1	i.

TABLE VII

THE EFFECT OF ALTITUDE UPON RADIATOR PERFORMANCE

[Heat dissipation and P_D are in hp./sq. ft. of openfrontal area; η_p , 100 percent, assumed for all values

of the exit setting; D, 1/48 ft.; L/D, 50]

FIGURE LEGENDS

(a) Static-tube connection.

(b) Sample tube.

Figure 1.- Tube for friction-loss study.

Figure 2.- Velocity distributions for the 1/2-inch-diameter circular tube.

Figure 3.- Pressure drop along a smooth tube with a streamline entrance.

Figure 4.- Summary of friction-loss data for single tubes.

Radiators				Single tubes	
Curve	Length (in.)	Tube diameter (in.)	L/D	Curve	L/D
A	18	0.240	75	D	75
B	9	.250	36	E	36
C	5	.125	40	F	40
G	23.7	.410	Corru- gated tube		

Figure 5.- Isothermal friction data for several radiators and comparison with single-tube data.

Curve	D (ft.)	Δp (lb./sq. ft.)
A	1/32	25.6
B	1/48	25.6
C	1/96	25.6
D	1/48	6.4

Figure 6.- Air velocity in the tube against length for several diameters. End losses included; T_a , 73.5° F.

Figure 7.- Analysis of single tubes.

Figure 8. Heat transfer against length for several tube diameters. $T_w - T_{ia} = 70^\circ$ F.; fully developed turbulent flow; Δp , 25.6 lb./sq. ft.

Figure 9.- Heat transfer against length for several values of Δp . $T_w - T_{ia} = 70^\circ \text{ F.}$; $D, 1/48 \text{ ft.}$

Figure 10.- Three-tube section from the corrugated-tube radiator.

- A, copper-coil secondary shorted.
- B, water pump.
- C, bypass.
- D, valve.
- E, expansion tank.
- F, orifice for measuring water flow.
- G, static tube, water manometer.
- H, venturi for measuring air flow.
- I, thermocouple installation.
- J, static tube, alcohol manometer.
- K, baffle plate.
- L, duct wall.
- M, radiator.
- N, expansion box.
- O, pitot tube, alcohol manometer.
- P, installations for nine thermocouples.

Figure 11.- Apparatus for heat-transfer investigation.

Figure 12.- Illustration of extrapolation to find h_a from h_t for one of the radiators.

Curve	Radiator length (in.)	Tube shape	Diameter (in.)
A	23.7	Corrugated	0.410
B	5	Round	.125
C	18	do.	.240
D	9	do.	.250
E	Recommended for fully developed turbulent flow by McAdams (reference 3, p. 173)		

Figure 13.- Correlation of the heat-transfer data.

Curve	D (ft.)	Δp (lb./sq.ft.)
A	1/32	25.6
B	1/48	25.6
C	1/96	25.6
D	1/48	6.4
G	Corru- gated tube	25.6

Figure 14.-- Heat transfer against length for several tube diameters. $T_w - T_{ia} = 70^\circ \text{ F.}$; end losses included; air constants taken at 73.5° F.

Figure 15.-- Cooling efficiency against length. $T_w - T_{ia} = 70^\circ \text{ F.}$; Δp , 25.6 lb./sq.ft.; f , 0.650; η_p , 100 percent; $\epsilon(C_{D_w}/C_L)$, 0.1; V_1 , 200 m.p.h.; V_2 , 300 m.p.h.

(a) Cooling efficiency against length for several values of Δp . $T_w - T_{ia} = 70^\circ \text{ F.}$; f , 0.750; η_p , 100 percent; $\epsilon(C_{D_w}/C_L)$, 0.1; V_0 , 300 m.p.h.; D , 1/48 ft.

(b) The choice of the design Δp . Data from table IV.

Figure 16.-- The choice of Δp for a duct installation.

Figure 17.-- The change in cooling efficiency with Δp . $T_w - T_{ia} = 70^\circ \text{ F.}$; f , 0.750; η_p , 100 percent; $\epsilon(C_{D_w}/C_L)$, 0.1; V_0 , 300 m.p.h.; D , 1/48 ft.; L , 0.75 ft.; T_a , 73.5° F.

Figure 18.-- Cooling efficiency against length for two pump efficiencies. $T_w - T_{ia} = 70^\circ \text{ F.}$; Δp , 25.6 lb./sq.ft.; f , 0.650; $\epsilon(C_{D_w}/C_L)$, 0.1; V_0 , 200 m.p.h.; D , 1/48 ft.

Figure 19.-- Cooling efficiency against length for various radiators with optimum free-area ratios. A, B, etc., as in table V; $T_w - T_{ia} = 70^\circ \text{ F.}$; Δp , 25.6 lb./sq.ft.; η_p , 100 percent; $\epsilon(C_{D_w}/C_L)$, 0.1; V_0 , 200 m.p.h.

Figure 20.-- The fluid conditions for a radiator in a duct.

Figure 21.-- The effect of altitude on the flow through the radiator. Fixed duct-exit opening; supercharged engine.

Figure 22.-- Illustration of the change in heat dissipation with altitude for a fixed exit opening.

(a) The cross-flow radiator.

(b) Possible frontal shapes for a given value of w_d .

Figure 23.-- The length of the path on the liquid side.

Figure 24.-- Effect of Δp on the cooling efficiency for an installation in a separate nacelle. $T_w - T_{ia} = 70^\circ\text{F.}$; f , 0.750; η_p , 100 percent; $\epsilon (C_{D_w}/C_L)$, 0.1; V_o , 300 m.p.h.; D , 1/48 ft.; C_{D_n} , 0.12.

(a) C_{D_n} , 0.12; no interference.

(b) C_{D_n} , 0.048; wing interference.

(c) C_{D_n} , 0.018; wing interference.

Figure 25.-- Cooling efficiency against length for an installation in a separate nacelle. A, B, etc., as in table V; $T_w - T_{ia} = 70^\circ\text{F.}$; Δp , 25.6 lb./sq.ft.; f , optimum for each tube shape and size; η_p , 100 percent; $\epsilon (C_{D_w}/C_L)$, 0.1; V_o , 200 m.p.h.

Figure 26.-- Frictionless duct, heating at constant pressure.

Figure 27.-- The pressure-volume cycle for the flow through a duct.

Figure 28.-- The analysis of the data on radiator weights from references 6 and 15.

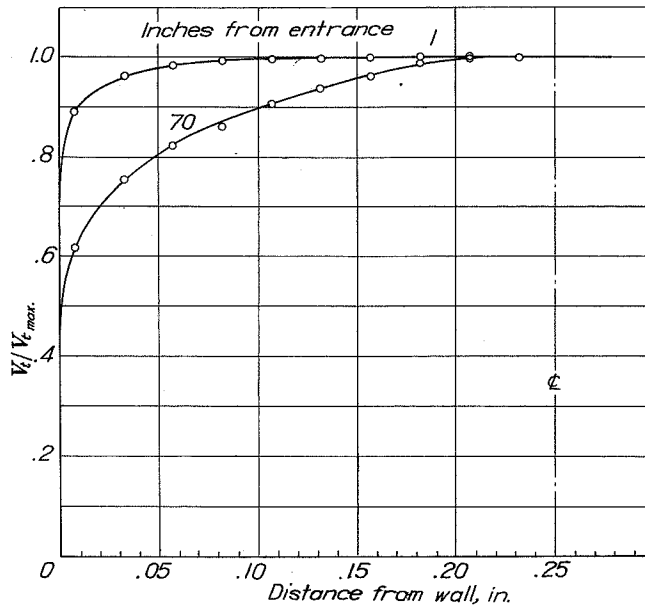
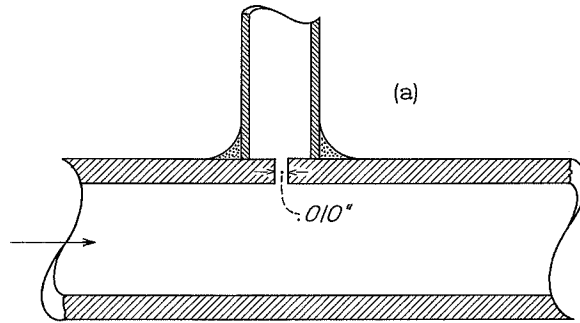


Figure 2

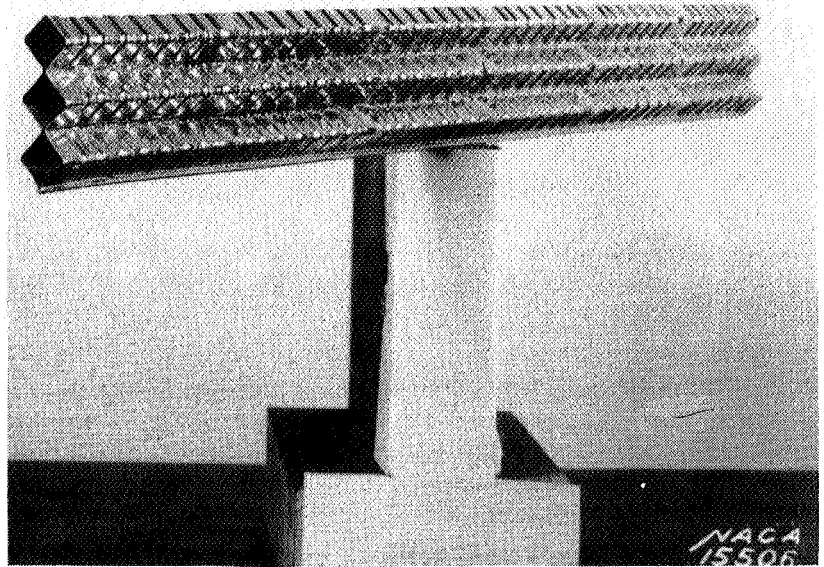
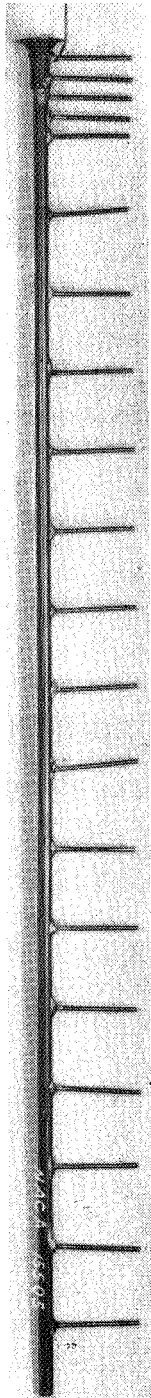


Figure 10.-- Three-tube section from the corrugated-tube radiator.

(b) Sample tube.

Figure 1.-- Tube for friction-loss study.

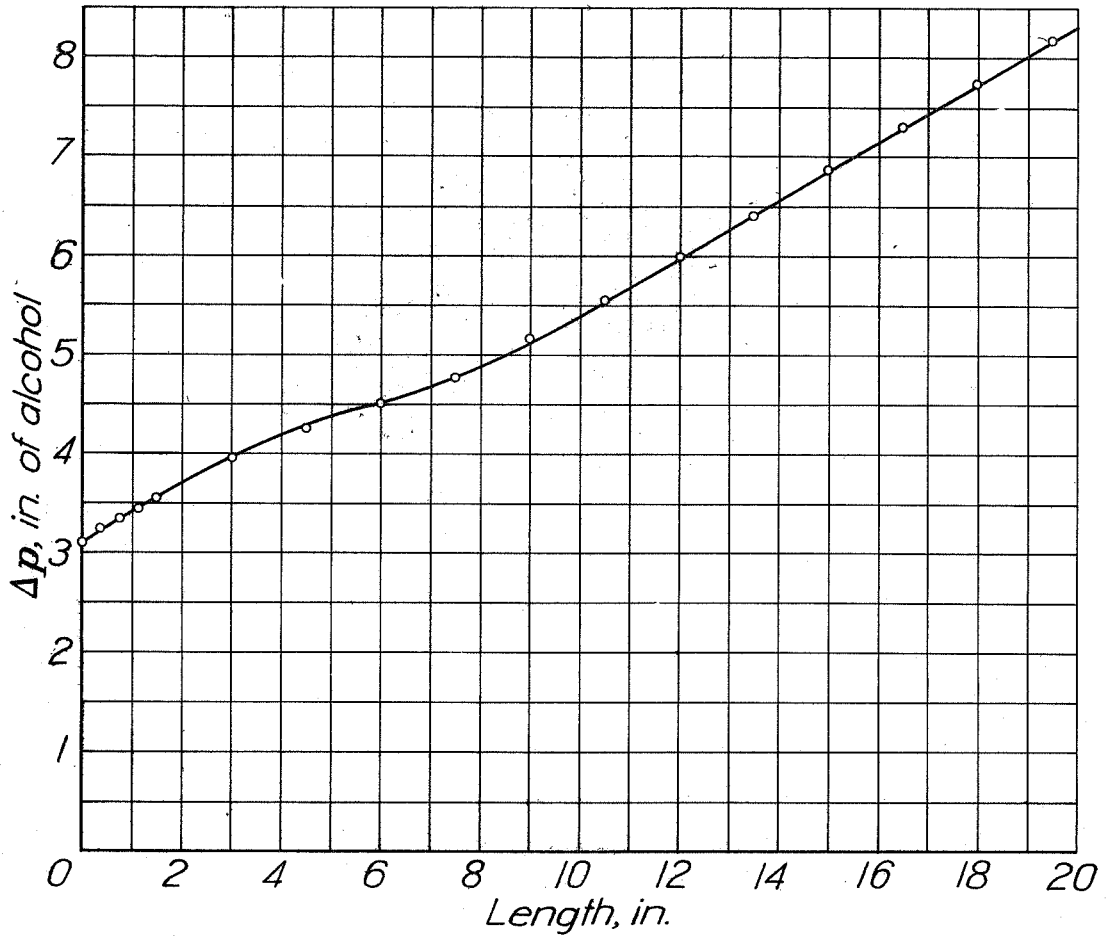


Figure 3

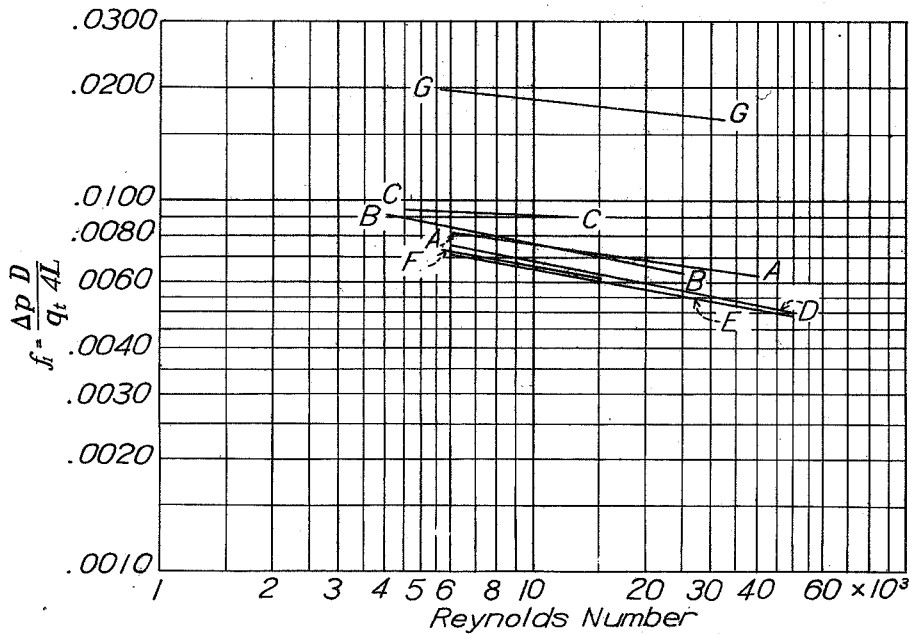


Figure 5

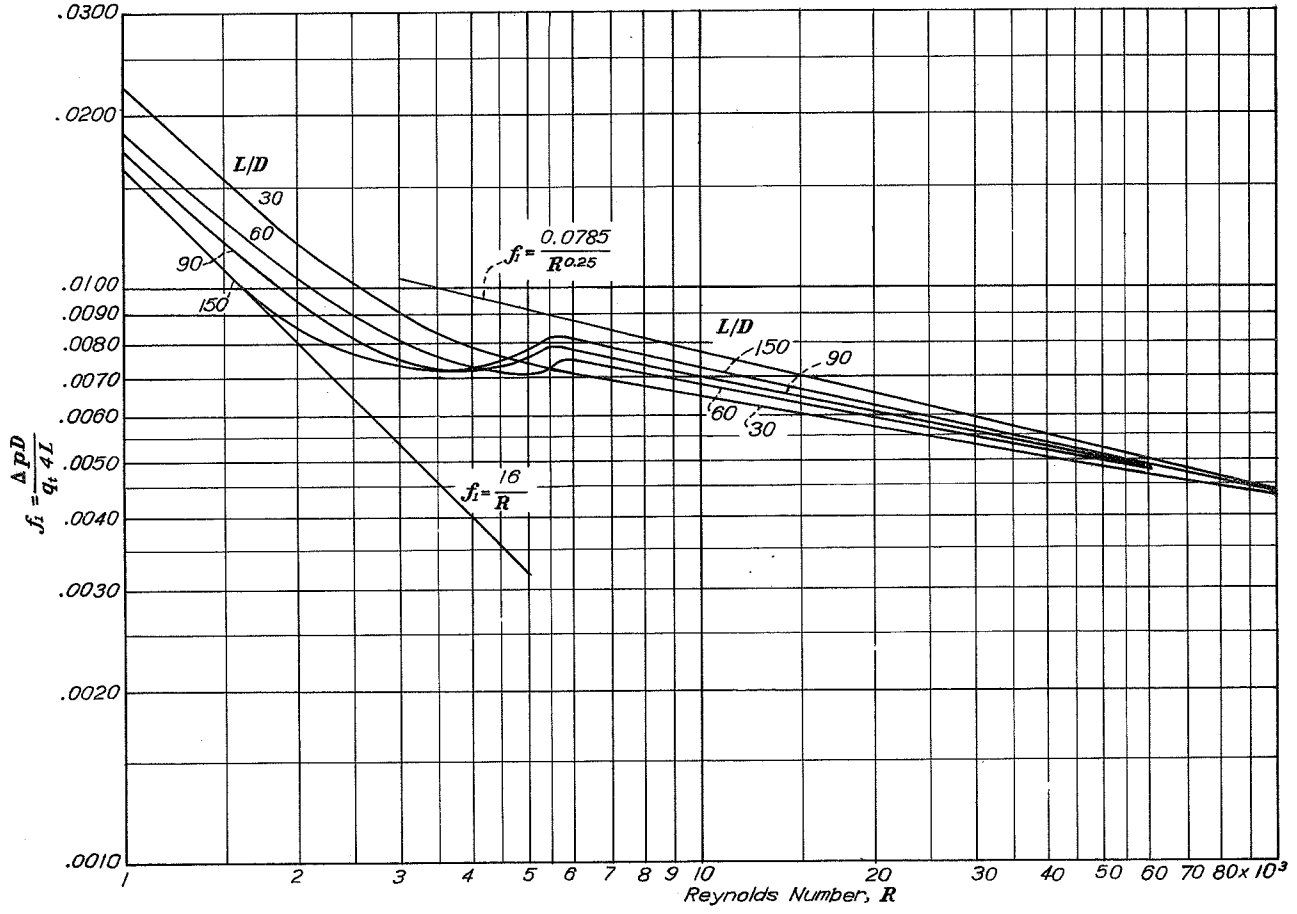


Figure 4

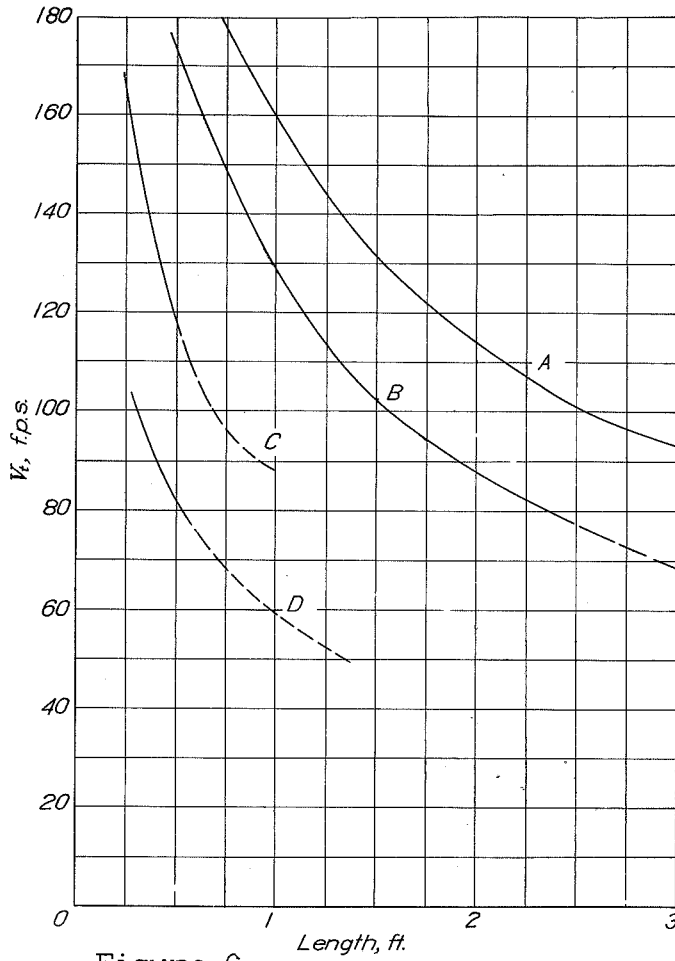


Figure 6

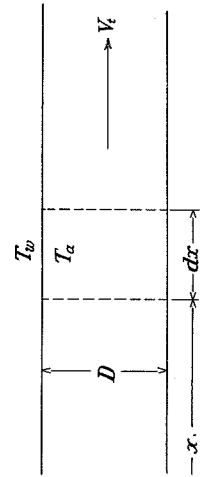


Figure 7

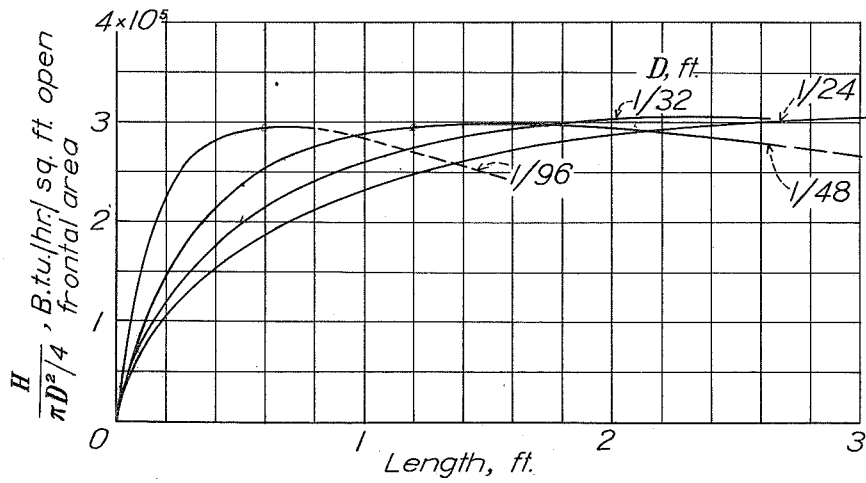


Figure 8

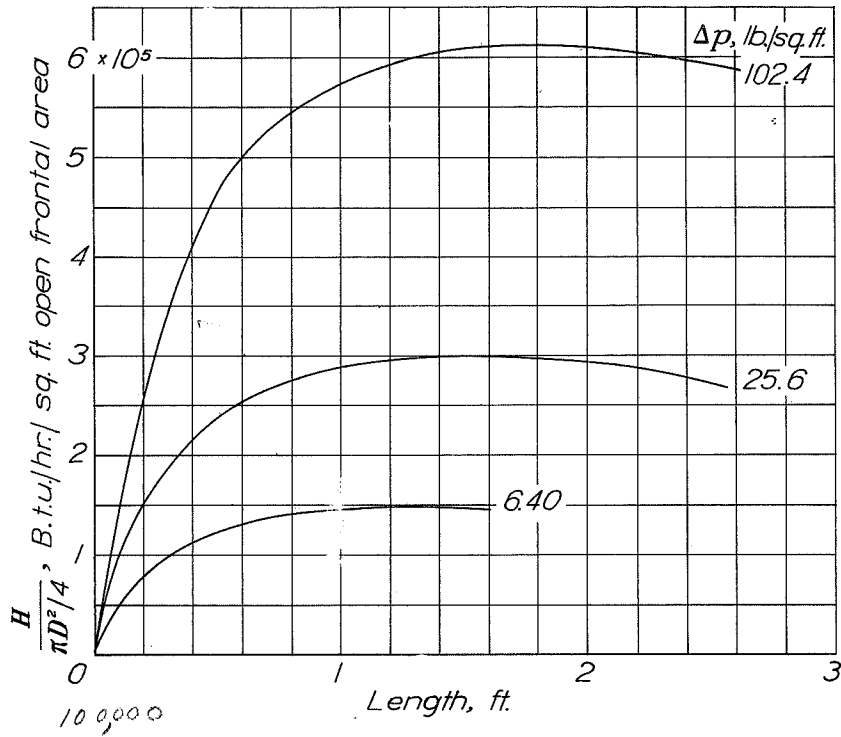


Figure 9

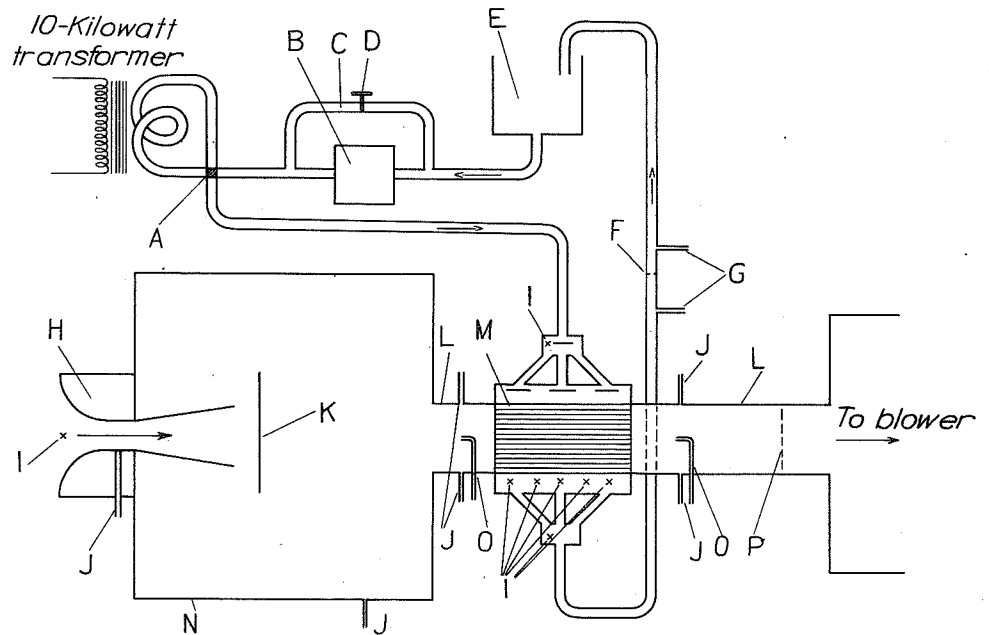


Figure 11

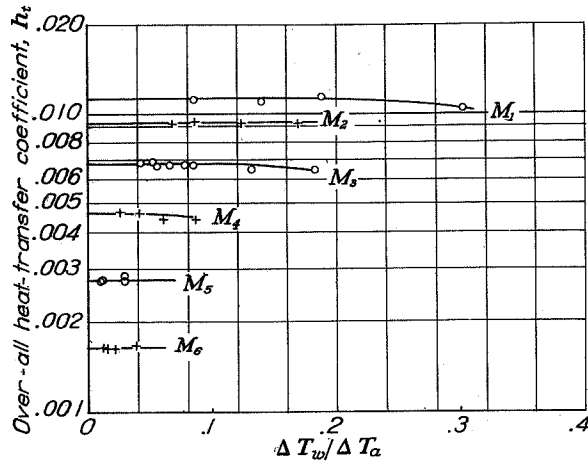


Figure 12

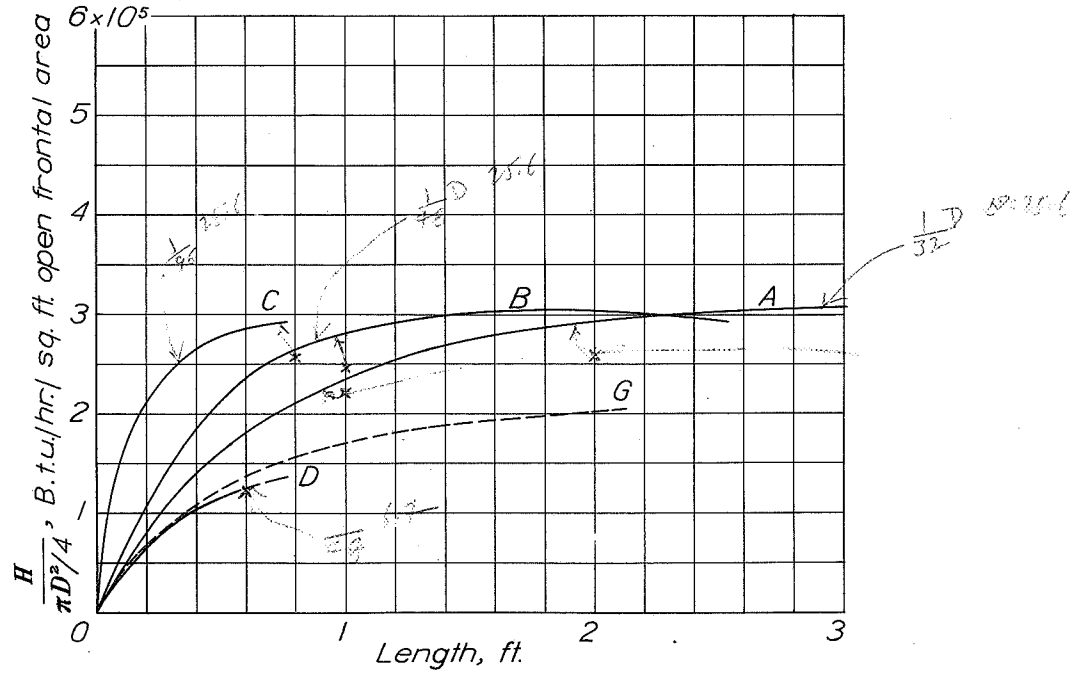


Figure 14

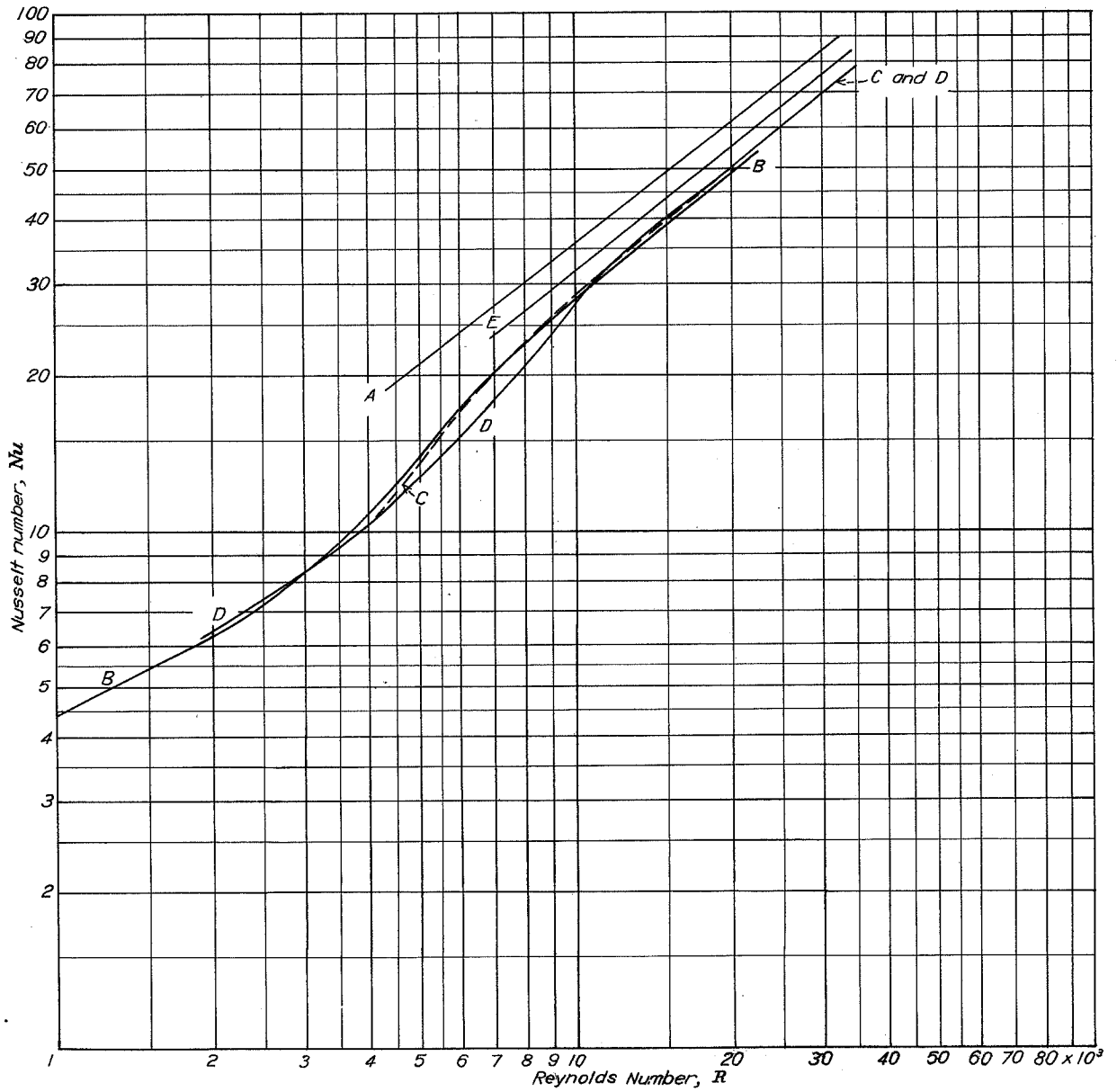


Figure 13

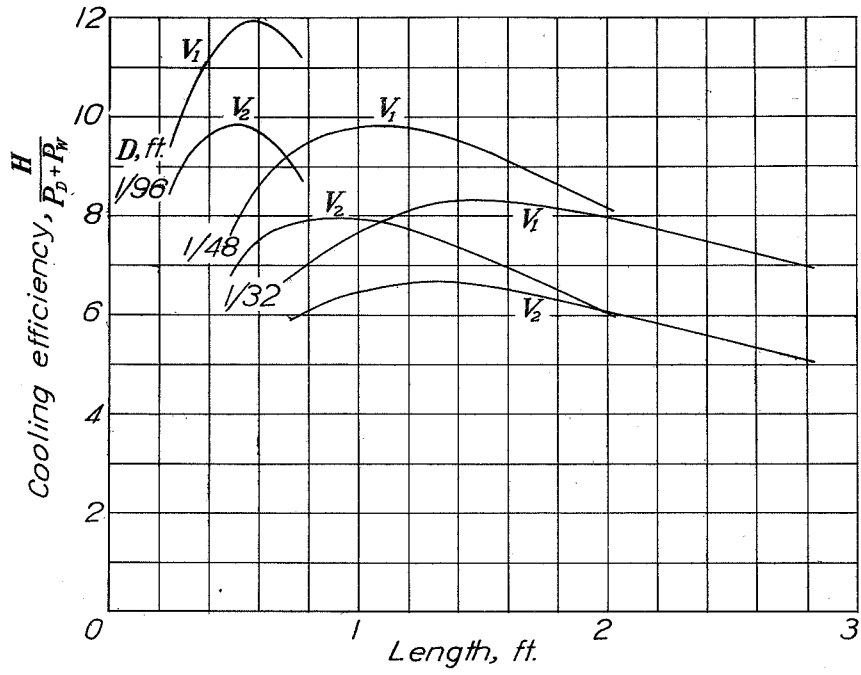


Figure 15

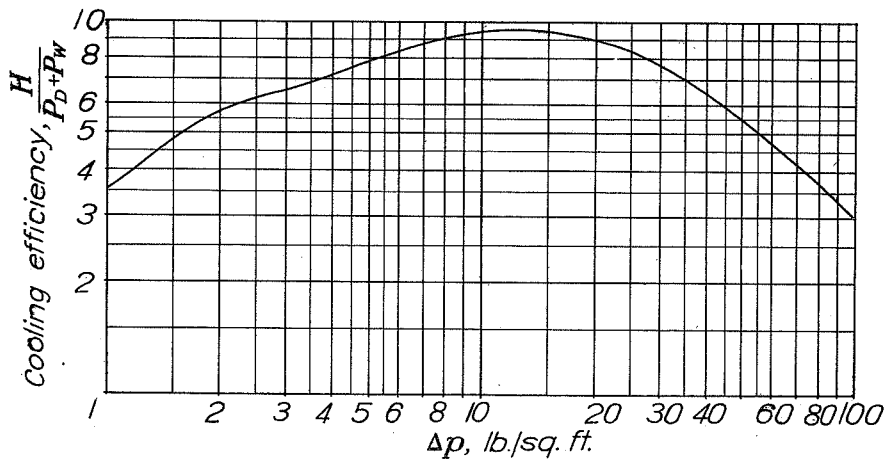


Figure 17

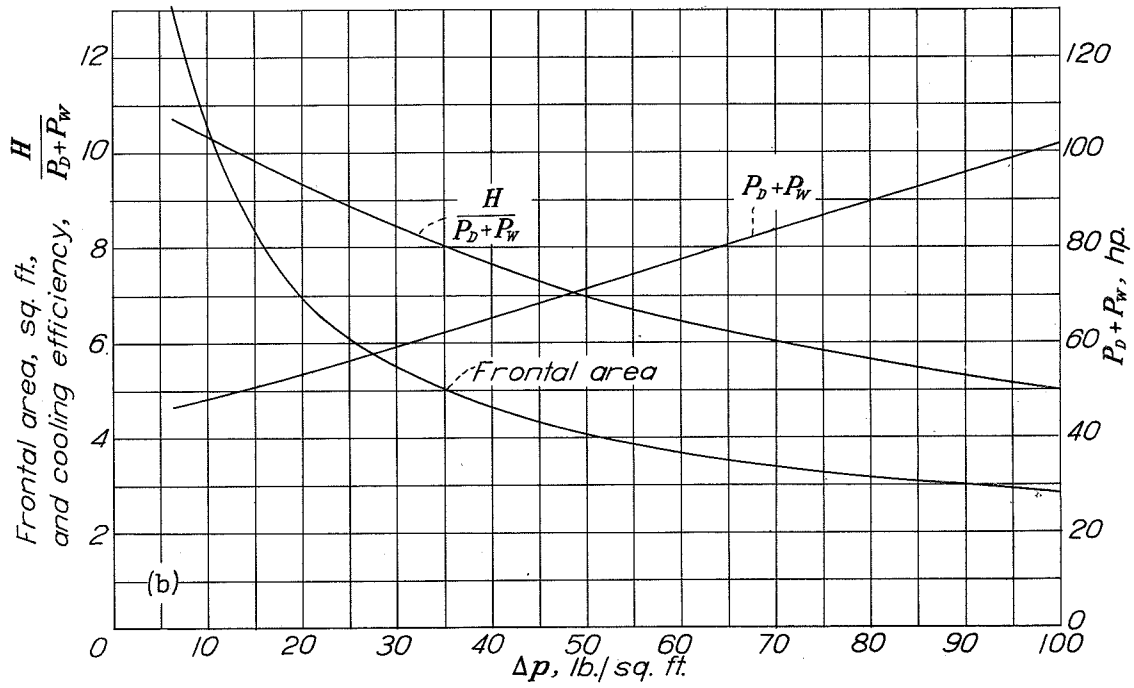
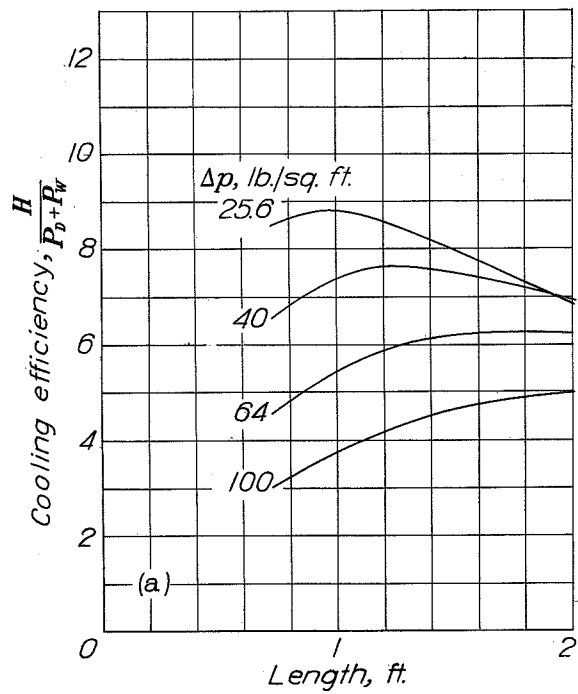


Figure 16

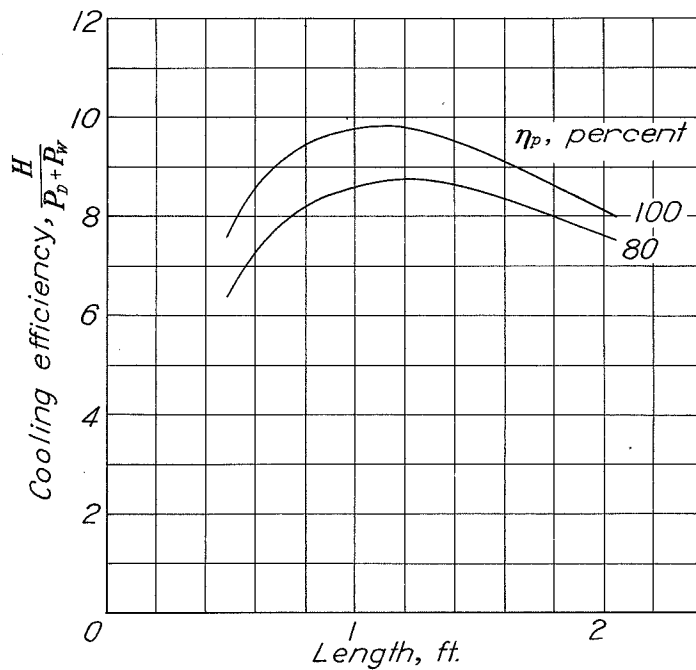


Figure 18

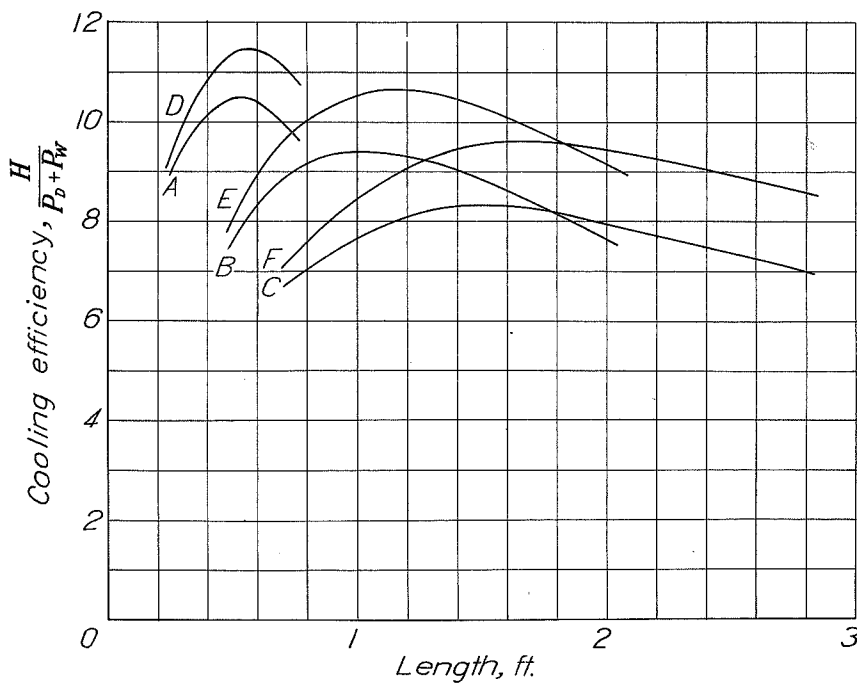


Figure 19

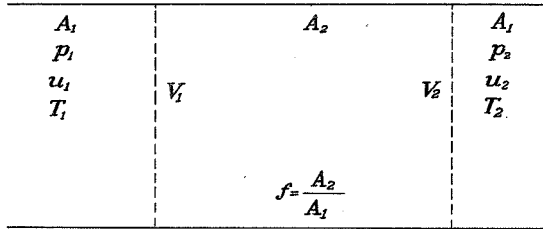


Figure 20

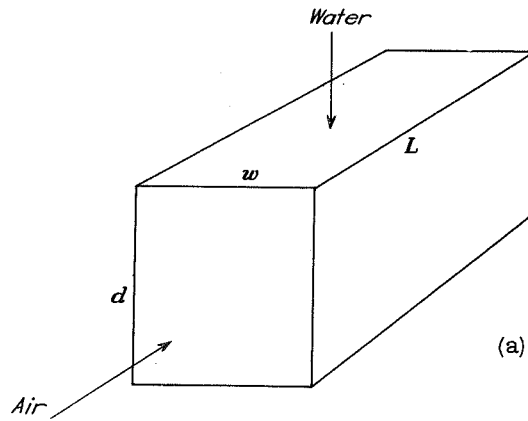


Figure 23a

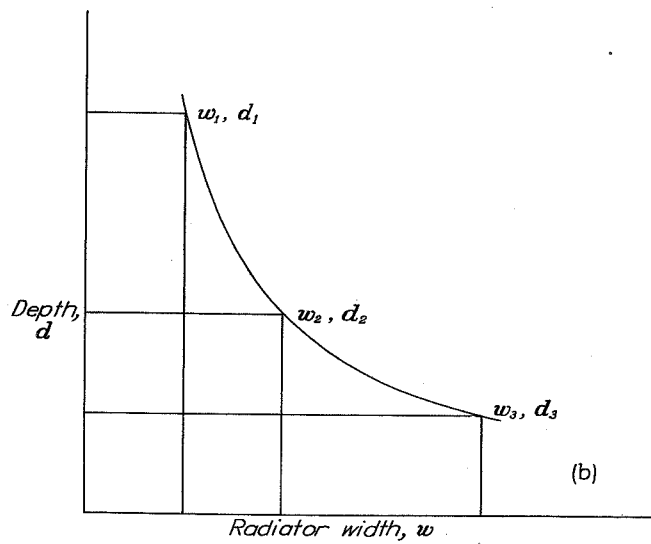


Figure 23b

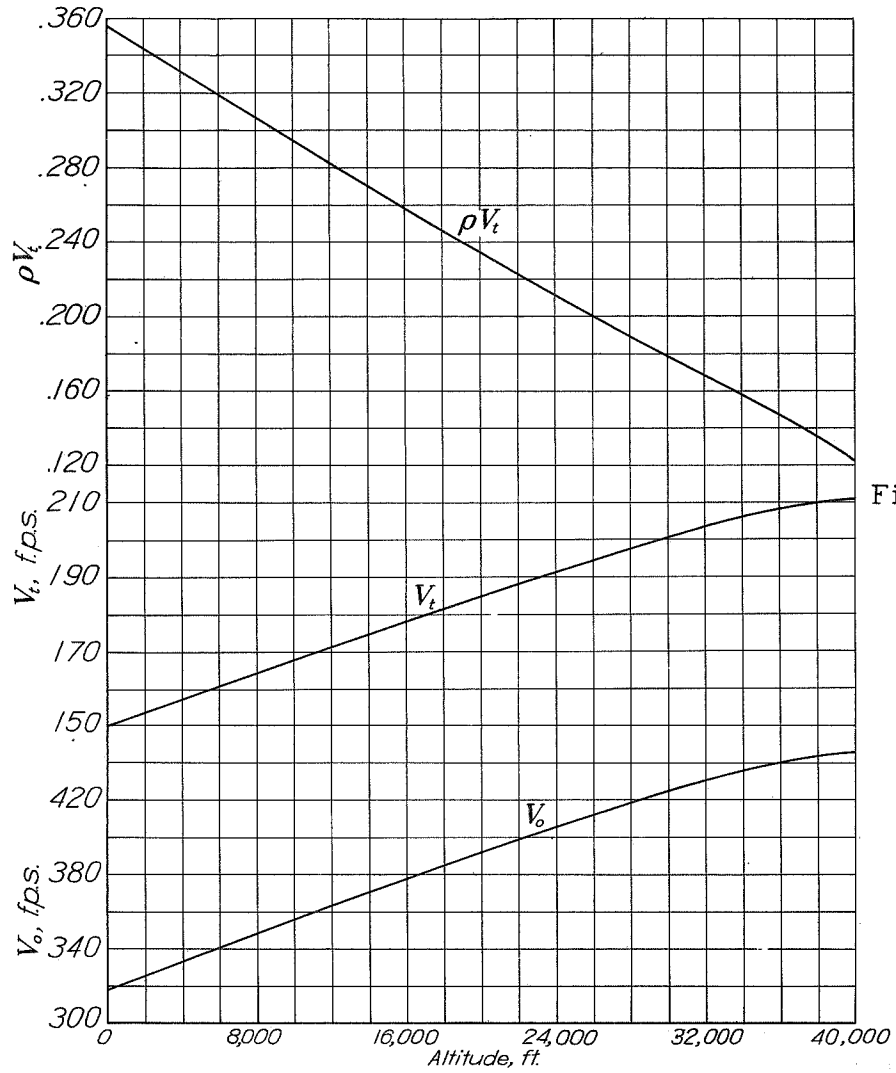


Figure 21

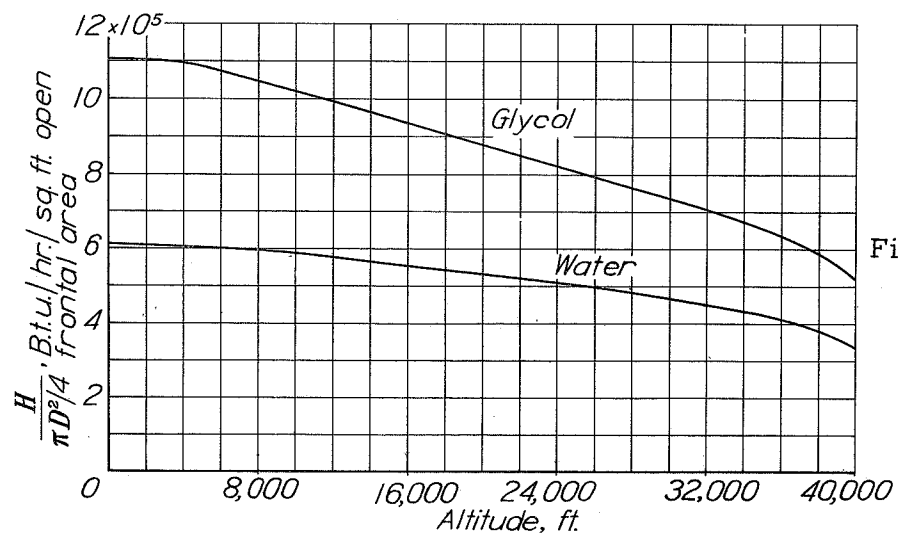


Figure 22

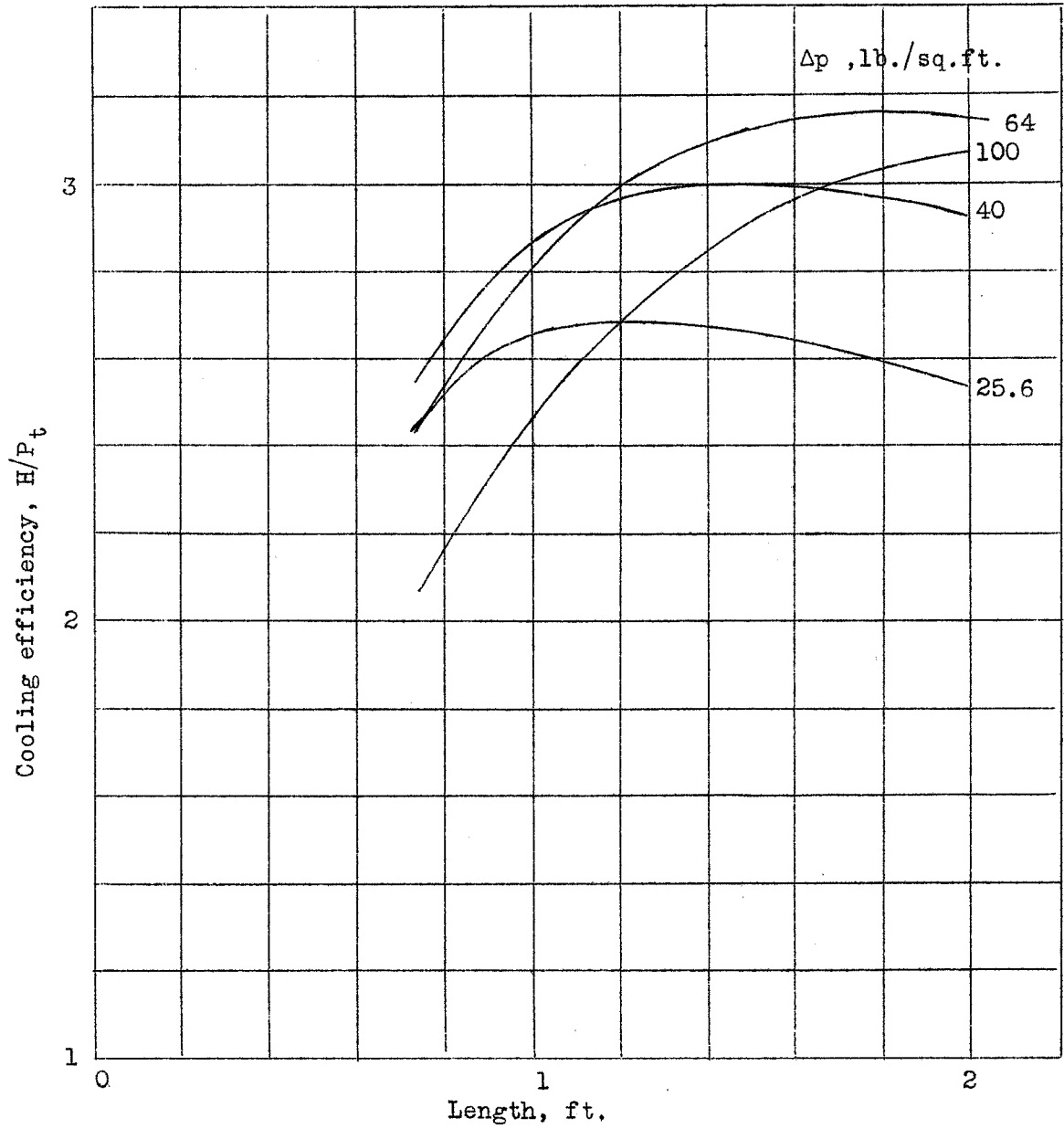


Figure 24

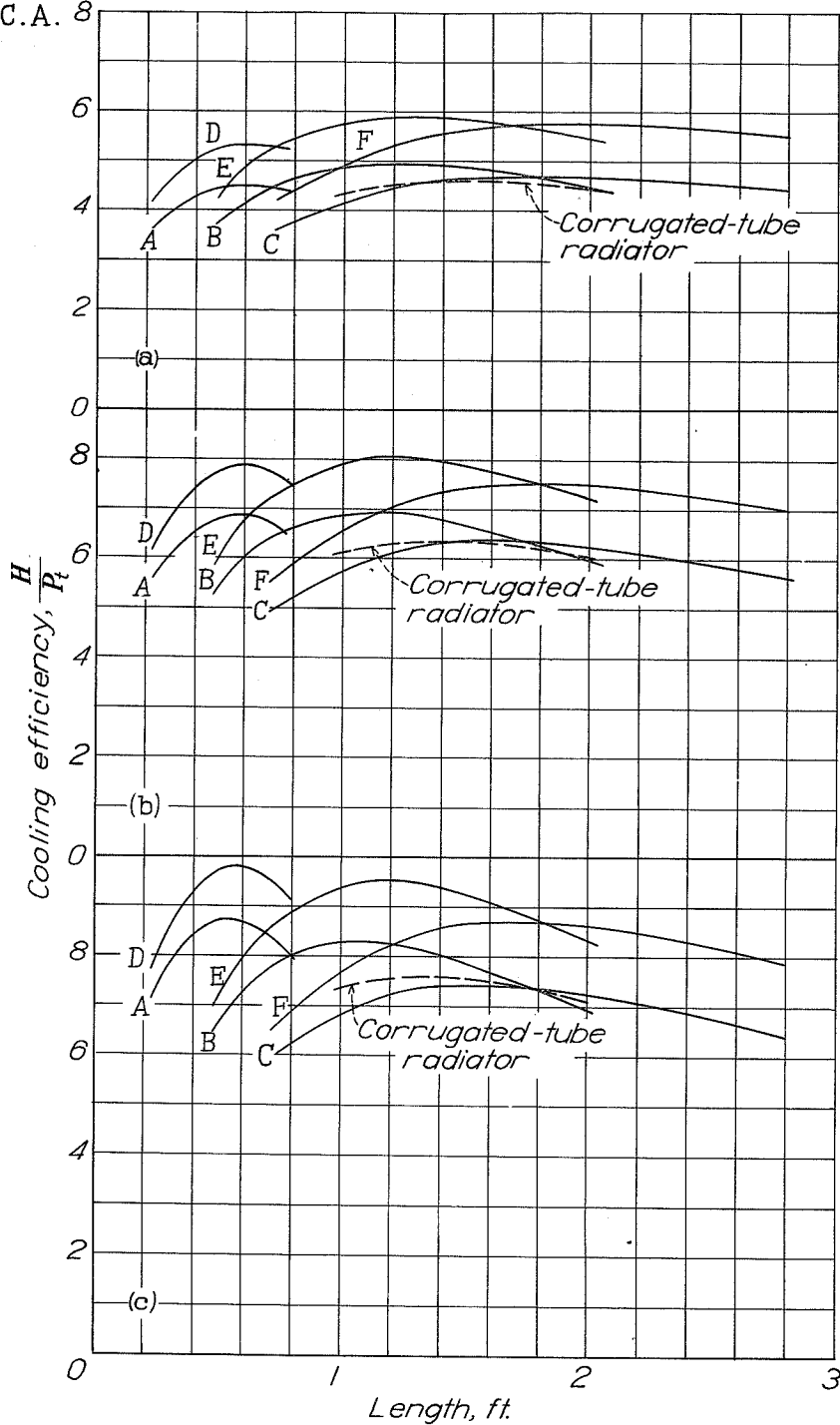


Figure 25

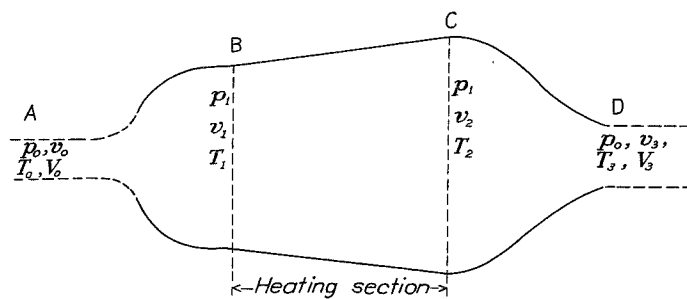


Figure 26

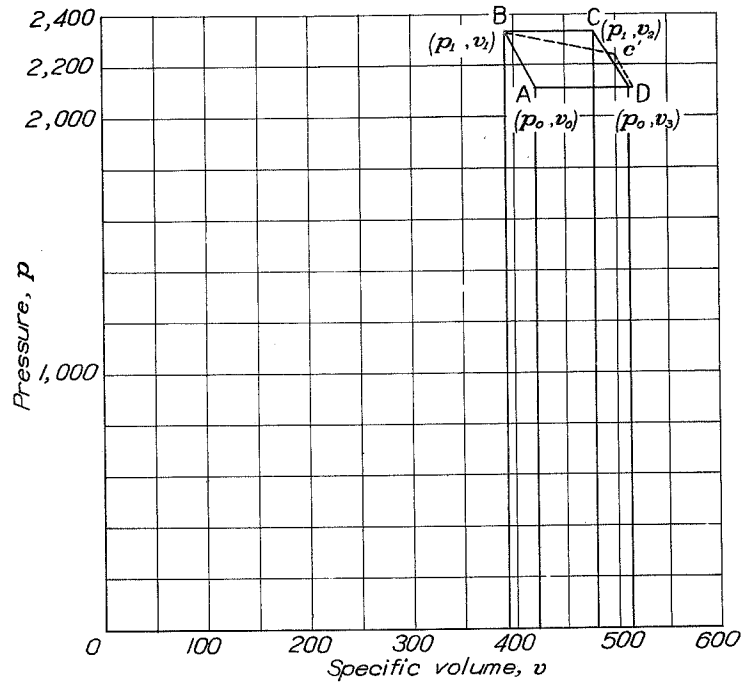


Figure 27

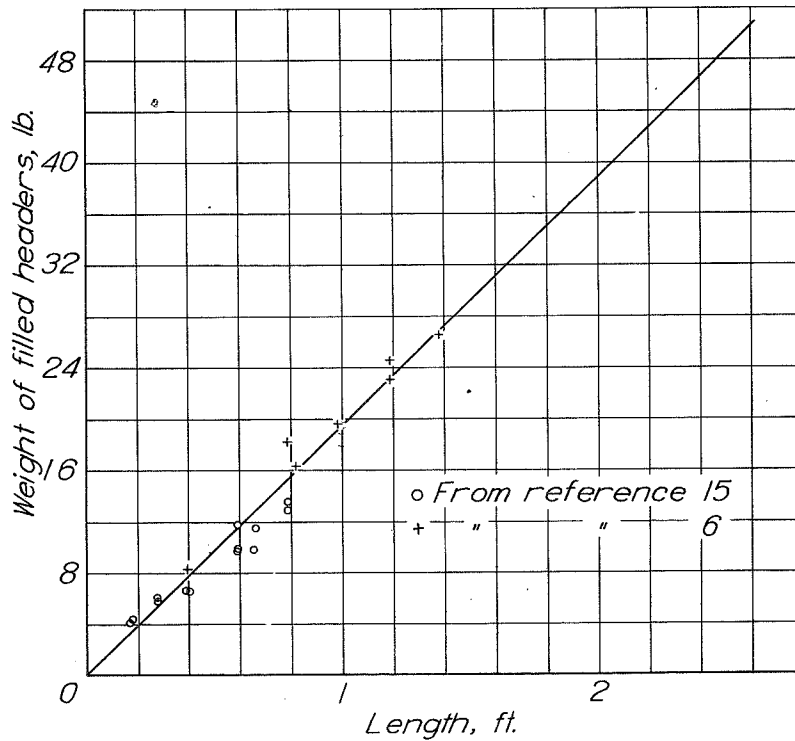


Figure 28